Geochemistry, Geophysics, Geosystems

RESEARCH ARTICLE
10.1029/2018GC008166

Special Section:
Clumped Isotope Geochemistry: From Theory to Applications

Modeling the Measurement: Δ_{47}, Corrections, and Absolute Ratios for Reference Materials

Gerard Olack[1] and **Albert S. Colman**[1]

[1]Department of the Geophysical Sciences, University of Chicago, Chicago, IL, USA

Abstract Clumped isotope studies on CO_2, Δ_{47}, that is the excess in the isotopologue containing both ^{13}C and ^{18}O at mass 47, can be very useful since they can give temperature estimates independent of the bulk isotopic composition. The measurement itself can be affected by a number of items. Here we develop a data processing model to examine the effects different interferences might have on the final calculated value. It incorporates known issues, for example, pressure baseline, ^{17}O excess, and shifts in absolute ratios for primary reference materials and parameters used for ^{17}O correction. We also included linearity effects as well as differences in isotopologue absolute abundances at a given m/z. What normally would be considered acceptable mass spectrometer ^{45}R and ^{46}R linearity can skew Δ_{47} results. That is 0.04‰/V and −0.04‰/V linearity on ^{45}R and ^{46}R respectively would also cause an apparent shift in the parameters used for ^{17}O corrections. Measurements were made on CO_2(g) equilibrated with water, and we were able to match up the effects seen with model results. Linearity and small differences in amplitude between sample and working reference gas affected Δ_{47} determination, as did apparent shifts in isotopologue abundances under different conditions. This may (partially) account for discrepancies seen in Δ_{47}-temperature calibrations curves between laboratories. We also developed an easy way to precisely calculate the $\delta^{13}C$ and $\delta^{18}O$ that works well in spreadsheets without the need for multiple iterations.

Key Points:
- Linearity and choice of absolute ratios for standards have similar effect on measurements
- Measurement model for $\delta^{13}C$, $\delta^{18}O$, and Δ_{47} available
- A simple way to calculate isotopic values from mass spectrometer measurements presented

Supporting Information:
- Supporting Information S1
- Data Set S1
- Data Set S2

Correspondence to:
G. Olack,
golack@uchicago.edu

Citation:
Olack, G., & Colman, A. S. (2019). Modeling the measurement: Δ_{47}, corrections, and absolute ratios for reference materials. *Geochemistry, Geophysics, Geosystems*, *20*, 3569–3587. https://doi.org/10.1029/2018GC008166

Received 2 JAN 2019
Accepted 23 MAY 2019
Accepted article online 31 MAY 2019
Published online 23 JUL 2019

1. Introduction

The measurement and applications of the abundance of multisubstituted isotopologues, "clumped isotopes," have advanced rapidly since the groundbreaking work done in John Eiler's laboratory at Caltech (Affek & Eiler, 2006; Eiler, 2007; Eiler et al., 2014; Eiler & Schauble, 2004; Ghosh et al., 2006; Wang et al., 2004). Clumped isotope measurements quantify the excess of isotopologues having more than one minor isotope, that is, the difference from the expected amount assuming stochastic distribution for the given bulk composition. The most common clumped isotope measurement, Δ_{47}, characterizes the cosubstitution of ^{13}C and ^{18}O minor isotopes in a single CO_2 molecule. The excess in the m/z 47 signal, Δ_{47}, mainly the $^{16}O^{13}C^{18}O$ isotopologue (Wang et al., 2004), reflects the temperature of formation/equilibration of the CO_2 or carbonate species. The signal can be from CO_2 freshly equilibrated with water at a given temperature or locked in the carbonate of a shell or mineral as long as they have not been altered. Data reduction routines for Δ_{47} calculations were developed (Affek & Eiler, 2006; Huntington et al., 2009) before the 2010 paper describing the new values for the ^{17}O and ^{18}O relationship (Brand et al., 2010) and used the previously accepted values (Gonfiantini et al., 1995) along with the updated value for $^{13}R_{VPDB}$ (Coplen et al., 2002).

A recent issue facing the clumped isotope community is the need to use the proper parameter set for ^{17}O corrections in CO_2 isotopic measurements. A mix of different parameter sets has been used in the past and different ranges for working standards have been used to correct Δ_{47} data. The choice of parameters for the ^{17}O and ^{18}O relationship will affect Δ_{47} determinations (Daëron et al., 2016; Olack et al., 2013; Olack & Colman, 2016; Schauer et al., 2016). Schauer et al. (2016) demonstrated the sensitivity of Δ_{47} to ^{17}O corrections using a series of sample measurements. Daëron et al. (2016) also modeled the effect and showed that using a different parameter set for ^{17}O corrections when processing model data will lead to correlation between Δ_{47} and the $\delta^{13}C$ and $\delta^{18}O$ differences. The currently recommended values (Brand et al., 2010) provide the best fit to the data in both of their studies. We did not see that in every case in our previous work (Olack et al., 2013; Olack & Colman, 2016).

The model system presented here was developed to highlight some of the practical issues that need to be addressed when making clumped isotope measurements on CO_2. It includes a convenient method to find

a numerical solution to the equation used to solve for ^{18}R as presented by Santrock et al. (1985). The features modeled include those that can be readily determined and corrected, such as pressure baseline correction (PBL, Bernasconi et al., 2013; He et al., 2012), linearity on ^{45}R and ^{46}R, and pressure balancing. It also includes features that are not or cannot be readily determined, for example, differences in isotopologue behavior in the source. It was also used to map out the effects of switching parameter sets used in the determination of isotopic values from CO_2 measurements and visualize the $^{17}R/^{13}R$ relationship mentioned by Brand et al. (2010), etc. The model was used to evaluate a series of CO_2-water equilibrated gas clumped isotope experiments. The differences between the model and experimental values were used to examine how different items, for example, variations in isotopologue absolute abundances and linearity effects, affected Δ_{47} results.

1.1. Notation

The notation for working with isotopes can be simplified for publication (Coplen et al., 2002). The notation in Brand et al. (2010) is followed here, though parentheses around the isotope and the element are not being used, for example, $\delta^{13}C$ instead of $\delta(^{13}C)$, consistent with earlier publications (Santrock et al., 1985). For clumped isotopes, that is Δ_{47} for excess m/z 47, the notation from the clumped isotope community is followed, though there are some differences, for example, ^{45}R and $^{47}\delta$ here versus R^{45} and δ^{47} in Dennis et al. (2011). The definition of Δ_{47}, which also includes excesses in ^{45}R and ^{46}R, is in equation (1) and the expected amount for ^{47}R, $^{47}R^{*}$, is in equation (2) (Affek & Eiler, 2006; Huntington et al., 2009).

$$\Delta_{47} = 1000\times\left(\left({}^{47}R/{}^{47}R^{*}-1\right)-\left({}^{46}R/{}^{46}R^{*}-1\right)-\left({}^{45}R/{}^{45}R^{*}-1\right)\right) \quad (1)$$

$${}^{47}R^{*} = 2\times{}^{13}R\times{}^{18}R + 2\times{}^{17}R\times{}^{18}R + {}^{13}R\times{}^{17}R \quad (2)$$

Isotopic measurements for the relative abundances of the minor isotopes ^{13}C and ^{18}O are reported as part per thousand, that is, per mil or ‰, differences from primary standards. Isotopic values will also be reported without ‰ symbol but are in per mil.

1.2. ^{13}C and ^{18}O Values

For ^{18}O, the scale is defined by the primary standard Vienna Standard Mean Ocean Water, VSMOW. The ^{13}C primary standard is NBS-19, a limestone, but the scale is defined by the virtual Vienna Pee Dee belemnite, VPDB. Traditional CO_2 measurements assume (i) a stochastic distribution of the minor isotopes among the various isotopologues and (ii) that there is a consistent ^{17}O to ^{18}O relationship. Mass spectrometer measurements on CO_2 give readings for m/z 44, 45, and 46.The ratios of m/z 45 and 46 to m/z 44 measurements normalized to a standard, ^{45}R and ^{46}R, can be used to calculate the $^{13}C/^{12}C$, $^{18}O/^{16}O$, and $^{17}O/^{16}O$ ratios, ^{13}R, ^{18}R, and ^{17}R, for the sample following the protocol outlined in Santrock et al. (1985):

$$-3\times K^{2}\times{}^{18}R^{2\lambda} + 2\times K\times{}^{45}R\times{}^{18}R^{\lambda} + 2\times{}^{18}R - {}^{46}R = X, X = 0 \quad (3)$$

$${}^{17}R = K\times{}^{18}R^{\lambda} \quad (4)$$

$${}^{13}R = {}^{45}R - 2\times{}^{17}R \quad (5)$$

The constants, λ and K, are listed in Table 1 under SSH for Santrock et al. (1985). Equation (3) is solved by adjusting ^{18}R and the rest of the ratios calculated from equations (4) and (5) (see also Tables A1 and A2 for a complete list of equations used to generate and process data, especially Table A2, lines 14–17).

The current International Union of Pure and Applied Chemistry, IUPAC, recommendations for λ and K values are also in Table 1 under BAC (Brand et al., 2010). The recommendations include a new protocol for $\delta^{13}C_{VPBD}$ calculations that avoids a numeric solution to equation (3). This was done both to have a calculation more amenable for use in a spreadsheet and because the $^{17}R/^{13}R$ is well constrained, allowing for analysis of the propagation of error (Brand et al., 2010; equations (6)–(8)).

Table 1
Parameter Sets for ^{17}O Corrections

Parameters	1985[a]	SSH[a]	GSR[f]	BAC[m]	A&B[p,q]
$^{13}R_{VPDB} \times 10^6$	11,237.2	11,237.2	11,237.2[g] 11,194.9[h]	11,180 ± 28[n]	11,237.2
$^{18}R_{VSMOW} \times 10^6$	2005.2[b]	2005.2[b]	2005.2[b]	[2005.2][b]	[2005.2][b]
$^{17}R_{VSMOW} \times 10^6$	373 ± 7[c]	402 ± 8[c]	379.9 ± 0.8[i]	[384.8][l]	386.7[p]
$‰(^{17}R_{VSMOW})_{BAC}$[r]	−31	45	−13	0	5
$^{18}R_{VPBD\text{-}CO2} \times 10^6$			2,079[g] 2,088.3[j]	2,088.35[j]	2,088.35[j]
$^{17}R_{VPDB\text{-}CO2} \times 10^6$			379.95[g] 387.95[j]	393.1 ± 0.9	395.11 ± 0.94
$\lambda \times 10^3$	516	516	516.4 ± 3.3[k]	528[o]	528[o]
$K \times 10^3$	9.20235[d]	9.9235[e]	[9.3940][l]	10.22461	10.27689
$^{17}R_{VPDB\text{-}CO2}/^{13}R_{VPDB}$			0.03381 0.03466	0.03516	0.03516
$^{17}R_{VSMOW}/^{13}R_{VPDB}$	0.03319	0.03577	0.03381	0.03442	0.03441
$‰(^{17}R_{VSMOW}/^{13}R_{VPDB})_{BAC}$[r]	−35.6	39.4	−17.8	0.0	−0.2

Note. Primary values bracketed if not directly reported in reference.
[a]Santrock et al., 1985. Two sets reported. "SSH" refers to the one commonly referenced, that is, the set that fits their CO_2-water equilibration experiments. [b]Value taken from Baertschi (1976). [c]Calculated in Santrock et al. (1985) from λ (referred to as α in original publication) and K values, $^{17}R = {}^{18}R^{\alpha} \times K$. [d]Calculated from Neir's analysis of oxygen (Nier, 1950). [e]As reported in Santrock et al., 1985, eliminates $\delta^{13}C$ covariance with $\delta^{18}O$. [f]Gonfiantini et al., 1995. Top line value(s) used. Different $^{17}R_{VPDB\text{-}CO2}$ than Allison et al. (1995). [g]From Craig (1953). [h]Computed from measured values for NBS-20 by Zhang and Li (1987), via Gonfiantini et al. (1995). [i]From Li et al. (1988). [j]Computed from V-SMOW value (Baertschi, 1976) by Gonfiantini et al. (1995) and Allison et al. (1995). [k]Via Gonfiantini et al. (1995), from Matsuhisa et al. (1978). [l]Calculated here from reported values for other parameters using equation (4): $^{17}R = K \times {}^{18}R^{\lambda}$. [m]Brand et al., 2010, current IUPAC recommendations. [n]Coplen et al., 2002, calculated from best measurement for NBS19 (Chang & Li, 1990). [o]Value reported by Barkan and Luz (2005), Landais et al. (2008), and Meijer & Li, (1998). [p]From Assonov and Brenninkmeijer (2003b) using values from Assonov and Brenninkmeijer (2003a). [q]Table not comprehensive, for example, Kaiser (2008) omitted. Also, references may list values by atom percent, not mole ratio, and for ^{13}C, values may be for NBS19 not Vienna Pee Dee belemnite (VPDB). Oxygen may be for Vienna Standard Mean Ocean Water (VSMOW) or VPDB-CO2. [r]Part per thousand difference from BAC parameter set values for $^{17}R_{VSMOW}$ or $^{17}R_{VSMOW}/^{13}R_{VPDB}$, for example, $‰(^{17}R_{VSMOW})_{BAC} = 1000 \times (^{17}R_{VSMOW\text{-}SSH}/^{17}R_{VSMOW\text{-}BAC} - 1)$, calculated here.

$$\delta^{13}C_{VPDB} \approx {}^{45}\delta_{sample} + 2 \times \left({}^{17}R/{}^{13}R\right)_{VPDB-CO_2} \times \left({}^{45}\delta_{sample} - \lambda \times {}^{46}\delta_{sample}\right) \quad (6)$$

with

$$\left({}^{17}R/{}^{13}R\right)_{VPDB-CO2} = 0.03516(8) \quad (7)$$

and

$$\delta^{18}O_{VPDB-CO2} \approx \left({}^{46}\delta_{VPDB-CO2} - 0.0021 \times \delta^{13}C_{VPDB}\right)/0.99924 \quad (8)$$

The approximation for $\delta^{13}C_{VPBD}$ will deviate by up to 0.026 from the numeric solution in their extreme cases, for example, 25.000 $\delta^{13}C_{VPBD}$ and −50.000 $\delta^{18}O_{VPDB\text{-}CO2}$ (Brand et al., 2010). The numeric solution, as presented here, will be used and will include the updated parameters. Comparisons between different parameters sets, which vary in $^{17}R/^{13}R$, will be done.

1.3. Clumped Isotope, Δ_{47}, Values

The measurement of clumped isotopes, isotopologues containing two (or more) of the minor isotopes in the same molecule are made in a similar fashion to traditional isotopes (Eiler, 2007). In working with CO_2, the *m/z* 47 signal is primarily the $^{18}O^{13}C^{16}O$ isotopologue, the $^{13}R \times {}^{18}R$ component in equation (2). The reference gas in the instrument is treated as the initial standard and is commonly referred to as the working gas (WG), and the measurements are made against the WG (Huntington et al., 2009), as shown in Table A2, lines 7 and 18 ($^{47}R_{meas}$,$‰ {}^{47}R_{sample}$).

The expected ^{47}R is calculated from ^{13}R, ^{18}R, and ^{17}R, assuming stochastic distribution of the isotopes (equation (2) and Table A2, line 18, $^{47}R_{calc}$; Huntington et al., 2009). The actual isotopic distribution is not stochastic. It varies with temperature leaving a slight excess of the clumped, mass 47, isotopologue at low, such as room, temperatures (Wang et al., 2004). The ^{47}R value is normalized to the working gas to give

$^{47}\delta_{sample}$. The excess of m/z 47 is normalized to the working gas too since that was used to both measure ^{47}R and calculate ^{13}R, ^{18}R, and ^{17}R (Table A2, lines 18,19).

If $\delta^{13}C$, $\delta^{18}O$, and Δ_{47} are calculated together, using the same parameter set, then there will not be an excess in either ^{45}R or ^{46}R. Only the ^{47}R excess component is needed in equation (1). This is because equations (3) to (5) assume a stochastic distribution of the isotopes. If $\delta^{13}C$ and $\delta^{18}O$ are calculated separately by a different means, such as using values as reported by the mass spectrometer software, or with a different parameter set, then the differences in the calculations will give rise to ^{45}R excess and ^{46}R excess values. Those differences also affect ^{47}R determination. In that case, calculating the full Δ_{47}, equation (1), is needed.

A series of standards, including CO_2 equilibrated with water at different temperatures and CO_2 heated in quartz tubes to 1000 °C, are run over a range of $^{47}\delta$ to correct the working gas scale and report Δ_{47} as the excess from the true stochastic distribution, yielding values reported on the Absolute Reference Frame (ARF; Dennis et al., 2011). The ARF is needed to correct for scale expansion due to instrument response, data processing, etc.

1.4. ^{17}O Effects on Δ_{47}

The effect of different ^{17}O parameters sets on the Δ_{47} determination comes in directly, via the ^{17}R component used in $^{47}R_{calc}$ (Table A2, line 18; $^{47}R^{*}$ in equation (2)), and indirectly via the ^{13}R calculation and the ^{17}O component of ^{45}R (equation (5) and Table A2, line 17). Switching the parameter sets used to calculate ^{17}O from ^{18}O will then affect the Δ_{47} results (Daëron et al., 2016; Olack et al., 2013; Olack & Colman, 2016; Schauer et al., 2016). Also, samples having a large, in magnitude, excess of ^{17}O, Δ_{17} or difference in ^{17}O from the expected value calculated in relationship to ^{18}O should also have an effect on Δ_{47} (Halevy et al., 2011). Luz and Barkan (2010) measured a series of different meteoric water samples that showed Δ_{17} range from −0.016 to 0.076, with evaporatively ^{18}O enriched samples relatively depleted in ^{17}O. Extraterrestrial samples can have larger in magnitude variations, for example, 0.8 Δ_{17} for Martian meteorites (Farquhar et al., 1998; Halevy et al., 2011).

1.5. PBL, Linearity, and Absolute Abundance Effects on Δ_{47}

The expected m/z 47 signal is orders of magnitude smaller than the m/z 46 and requires more amplification to be detected (Ghosh et al., 2006). That also means it is more sensitive to interferences, such as abundance sensitivity, the main ion peak bleeding into the m/z 47 cup, and secondary electrons, electrons kicked off of surfaces when struck by an ion (Bernasconi et al., 2013; Fiebig et al., 2016; He et al., 2012). The PBL correction determined by measuring the off peak baseline while CO_2 is entering the source removes much of the problem (He et al., 2012). The residual baseline will still give rise to a much smaller Δ_{47} versus $^{47}\delta$ correction.

Linearity issues, namely, changes in ^{45}R and ^{46}R with changes in m/z 44 signal intensity, affect $\delta^{13}C$ or $\delta^{18}O$ values (Mook & Grootes, 1973). Those issues will affect Δ_{47} determination. The sensitivity of Δ_{47} to linearity effects on the other species, m/z 45 or m/z 46, is modeled directly. Linearity is also broken down into its component parts, that is, changes in m/z 44, 45, and 46 responses with changing intensity, though the input for the model is still in ^{45}R and ^{46}R. A linearity effect on m/z 44 will affect both ^{45}R and ^{46}R linearity values since m/z 44 is in the denominator. A linearity effect on m/z 47 will show up as a Δ_{47} versus $^{47}\delta$ trend, corrected in part by the empirical transfer function (ETF) when values are mapped on to ARF, and has been a main focus of the clumped isotope community (Dennis et al., 2011). The present work assumes that there will be a Δ_{47} versus $^{47}\delta$ correction and will not focus on that.

Instrument suppliers usually rate the linearity of their instruments to be better than some small value. For Thermo instruments used in this study, it is typically <0.06‰/V for ^{45}R and ^{46}R measured against changes in amplitude for m/z 44. Clumped isotope measurements are in the 12 to 16 V range for m/z 44. If reference gas and sample pressures are not balanced, or if they have different $\delta^{13}C$ and $\delta^{18}O$ values, different signal strengths on m/z 45 and/or 46 will occur and the linearity will affect the modeled or calculated value. Errors in $\delta^{13}C$ and $\delta^{18}O$ will translate into differences in the expected $^{47}\delta$ and affect the Δ_{47} result. If the pressure difference results in a 1 V difference in signal, then 0.05 shifts could be seen for $\delta^{13}C$ and $\delta^{18}O$. Large differences in $\delta^{13}C$ or $\delta^{18}O$ from the WG will mean differences in m/z 45 or 46 at the same voltage on m/z 44, for example, a difference of 50‰ $\delta^{18}O$ is ~1 V difference at 20 V on m/z 46, whichcould lead to a shift in the $\delta^{18}O$ value.

Using different ^{17}O parameter sets for $\delta^{13}C$ correction affects the calculated amount of the $^{17}O^{12}C^{16}O$ isotopologues, ^{17}R in equations (4) and (5), which compose the m/z 45 signal. The ^{17}O correction presupposes that those isotopologues have the same absolute abundance, gas molecules per ion detected, as the main m/z 45 component, $^{16}O^{13}C^{16}O$. If they were different, that would be expected to give rise to an apparent shift in ^{17}O parameter set. Work on NO_2-NO systems indicates that the parent isotopologues do not give rise to the expected daughter NO ions at the same rate (Westley et al., 2007). One possibility is that the parent isotopologues break down at different rates, meaning the parent species could have different absolute abundances. The potential for different isotopologues at the same m/z to have different absolute abundances was added in to our model system as fractional isotopologue absolute abundances (FI, appendix Table A1, lines 14–16), so the effects could be assessed. Source scrambling and sample contamination have not been included in the model. The former is expected to be small (Yeung et al., 2012), corrected by projecting results onto the absolute reference frame (Dennis et al., 2011), and may already be included in the model. The PBL effect was initially attributed to source scrambling (He et al., 2012). Sample contamination should vary by individual sample run, with contaminated samples being flagged as outliers.

2. Materials and Methods

2.1. Model measurements

The model system can be found in two spreadsheets in the supporting information, with the equations listed in order in the appendix, Tables A1 and A2. It consists of first calculating the ^{13}R, ^{18}R, and ^{17}R values for CO_2 from a given set of $\delta^{13}C$ and $\delta^{18}O$ values using the equations and the reported absolute ratios for the standards (see Table A1, lines 1–4). These are converted into fractional amounts. The fractional amount of the masses, ^{44}F, ^{45}F, ^{46}F, and ^{47}F, composed of the different molecular species can be calculated (Table A1, lines 5 to 16) assuming stochastic distribution, with corrections for Δ_{47} applied (Table A1, lines 11–13). This is done for both the designated WG reference and the model sample runs. Multiplying them by a target signal value and relative amplification of the different measuring cups will return the model m/z readings for 44, 45, 46, and 47 (Table A2, lines 1–6). Modifications can then be made to the sample ratios or m/z readings to study different effects, for example, linearity (Table A2, lines 2 and 5). The parameter set used to calculate the isotopic composition from the model data set can be different from that used to generate the model data set (Table A2, lines 9–11).

Other modificationsinclude shifting the $\delta^{13}C$ and $\delta^{18}O$ values for the WG, applying FI changes at a given m/z value, incorporating ^{17}O excess (Table A1, line 4), changing the baseline, changing the signal strength between samples and WG, and applying linearity effects (Table A2, lines 1–6). At natural abundance levels, a primary species, consisting of a mixture of ^{12}C, ^{13}C, ^{16}O, and ^{18}O, dominates each m/z. The main ^{17}O containing species are minor species, and for m/z 45, 46, and 47, constituting 6.6%, 0.2%, and 3.4% of the signal, respectively (Kaiser, 2008). Those components each have a multiplier, FI, to account for fractional isotopologue absolute abundances (Table A1, lines 14–16). The theoretical calculations for Δ_{47} also include Δ values for each isotopologue, which can also be incorporated into FI multiplier for the main ^{17}O isotopologues (200 K calculated values, Wang et al., 2004) at a given m/z:

$$\mathrm{FI}_{m/z} = 1 + \frac{\Delta_{m/z}}{1,000}; \left(\Delta_{^{16}O^{12}C^{17}O} = -0.0117; \Delta_{^{16}O^{13}C^{17}O} = 0.9347; \Delta_{^{17}O^{12}C^{18}O} = 0.4674\right) \quad (9)$$

The baseline effects can be added to or subtracted from the model voltage data (Table A2, line 4). The changes in signal strength means changing the target value of m/z 44 for the samples, with the exact response for a given m/z dependent on the ratio calculated for that m/z. Linearity is typically reported as change in ^{45}R and ^{46}R with signal strength on m/z 44, ‰/V, adjusted by changing gas pressure in the source, and thus the readings in the cups. For the model, it is converted to per mil change per 1,000 mV change at a given m/z, for example, 45, using the ratios of the working reference gas, $^{45}R_{WG}$ in this case. The per mil shift in signal strength is determined by the difference in the signal strength between the reference gas and the sample at a given m/z and applied to the model signal (Table A2, line 2 and 5). It is being treated as a traditional calibration line. If a linearity correction is applied to m/z 44 and another species, for example, ^{45}R, then the effects would combine.

The model readings are treated as real data in order to calculate the $\delta^{13}C$, $\delta^{18}O$, $\delta^{17}O$ (from ^{18}O), $^{47}\delta$, and Δ_{47}(Huntington et al., 2009; Santrock et al., 1985). One of the model $\delta^{13}C$, $\delta^{18}O$ sets is designated as the WG. The m/z 45/44, 46/44, and 47/44 ratios of the designated WG and model samples are taken, then the sample ratios are normalized to the designated WG (Table A2, lines 7–8). Since the designated WG is, by definition, known, its ratio of masses can be calculated as was done above from the reported $\delta^{13}C$ and $\delta^{18}O$, assuming stochastic distribution (Table A2, lines 9–14). Multiplying the sample ratios by the calculated WG ratios gives their absolute ratios (Table A2, lines 12–14).

From the ratios, $^{18}R_{sample}$ can be calculated from equation (3), adjusting the ^{18}R value in equation (3) until X equals 0. The initial value for ^{18}R, $^{18}R_{init}$ is estimated from ^{46}R by dividing by 2 since $^{18}O^{12}C^{16}O$ is the main component m/z 46 (Kaiser, 2008). The result from equation (3), X, using $^{18}R_{init}$ can be divided in half and subtracted from the initial ^{18}R value to generate a better ^{18}R estimate. The values will converge after three to five cycles. The protocol was optimized, using equation (10) for $^{18}R_{init}$, then equations 3 and (11) (Table A2, lines 14–15).

$$^{18}R_{init} = {}^{46}R/2.005 \tag{10}$$

$$^{18}R_{final} = {}^{18}R_{init} - X/2.0022 \ \left(X \le 1E-9 \ \text{ using } {}^{18}R_{init} \ \text{ in equation 3}\right) \tag{11}$$

^{17}R is then calculated from ^{18}R, and ^{13}R is calculated from ^{45}R and ^{17}R using equations (4) and (5). Different parameter sets can be used (Table 1), and X will still be <1E−9. The isotopic and clumped values are calculated from the data supplied by the model, with the clumped isotope, Δ_{47}, is normalized to the WG (Table A1 for model data generation, Table A2 for processing).

With the model system, all parameters do not have to be kept the same. The model data can be calculated using one parameter set and then processed with another, mimicking the effect of processing real data with an incorrect parameter set (Table 1). This is fundamentally different then processing data with two different parameter sets, one for $\delta^{13}C$ and $\delta^{18}O$ determination and a second for Δ_{47} using equation (1). The model is generating data to be processed. Since it is a model system, each parameter can be varied individually, either for data generation or processing.

Model tests were typically done using a matrix of $\delta^{13}C$ and $\delta^{18}O$ values, 0 to −50 and 0 to +50 respectively, step size 10. One of the matrix data points may be shifted or one of the step sizes removed to help keep track of the data points when plotted. The model data was set to 16 V (16,000 mV) for m/z 44 (if 100% $^{12}C^{16}O^{16}O$), and the relative amplifications for m/z 45, 46 and 47 were 100, 333, and 3,333, respectively. The isotopic range therefore covers ~1 V on m/z 45 and 46. The WG in the model was −3.61‰ $\delta^{13}C_{VPBD}$, 24.99‰ $\delta^{18}O_{VSMOW}$, our OzTech tank value (section 2.3), or 0‰ $\delta^{13}C_{VPBD}$ and 0‰ $\delta^{18}O_{VSMOW}$, 0‰ $^{47}\delta$, and 0‰ Δ_{47}. Other settings used too, for example, 0.9 and 0.5 Δ_{47} for WG and sample matrix, respectively. In the series of tests presented here, the values for the working reference gas are set. Note that not all possible model tests are described here.

The model system can also be used to fit measured data, e.g. the equilibrated gases described in section 2.2. The $\delta^{13}C$ and $\delta^{18}O$ values from the reference gas and sample runs, and the parameter set from the measurement, are used for model input. The sum of the squares of the differences between the model Δ_{47} and the sample Δ_{47} values is minimized when fitting designated parameters, along with sample Δ_{47} and PBL_{47} (m/z 47 baseline). For these studies, the samples varying in $\delta^{13}C$ and $\delta^{18}O$ are prepared to have the same Δ_{47}, but the exact value relative to the WG is not known. The fitting to PBL_{47} is carried out since there will be a residual baseline even after off-peak measurement and correction to PBL_{47} (He et al., 2012). This can be done in Excel (Microsoft Corporation, Redmond, CA) using the solver function (GRG nonlinear, minimize the value in the cell that is the sum of squares of the differences by modifying parameters of interest, allow cells being modified to go negative). Constraints can be placed on the designated parameters being fit if needed. Different parameters may effectively modify the same variable(s), such as the FI series and Δ_{17}, so they have to be treated separately. Spreadsheets for the matrix model and processing experimental data are provided in the supporting information.

2.2. Equilibrated Gas Measurements

Mass spectrometric measurements made in this study were conducted on CO_2 equilibrated with water (equilbrated gas, EG) at 26 °C, and a series of samples were generated spanning a range of $^{47}\delta$ so each set

can be used to calculate its own empirical transfer function (ETF), a Δ_{47} versus $^{47}\delta$ correction (Dennis et al., 2011). Initial experiments were done using house waters, EG1, or recently acquired SLAP and VSMOW2, EG2. The protocol presented in He et al. (2012) was followed and is briefly described here. Approximately 200 to 300 μl water was loaded into a borosilicate glass tube (4-mm ID, 25- to 30-cm long), frozen in the tip using liquid N_2 (LN2), attached to a vacuum line (Wilmad-Labglass, Chicago, IL), the cooling bath was switched to a LN2-ethanol slurry (−80 to −100 °C) and the tube evacuated. The cooling bath for the tube was switched back to LN2, and approximately 15 μmol CO_2 gas was frozen over to the tube, and any residual noncondensable gases pumped away. Tubes were then flame sealed (final length ~15–20 cm) and placed in a 26 °C incubator for greater than 24 hr. When needed, a tube was removed from the incubator, the water shaken down to one end, and the CO_2 and water were immediately frozen down in one tip using LN2. The tip was slowly lowered into the LN2 as the ice formed to prevent breaking the tube. The tip of tube was then placed in a slurry bath, the top scored and loaded into a tube cracker. The line was evacuated and the sample tube cracked, allowing the CO_2 to be passed through a water trap (LN2-ethanol slurry) and frozen into the CO_2 trap using LN2. Any noncondensables were noted and pumped away. The CO_2 was then frozen into transfer vessels (tube with Kontes Hi-Vac valve, Kimble Chase, Rockwood, TN) and loaded into the mass spectrometer for isotopic measurements. Note that earlier tests using house water samples indicated further sample cleanup is not necessary, which saves time and avoids potential fractionation during sample clean up.

These experiments were repeated, EG3, using house waters and older stocks of SLAP, GISP, and VSMOW using 5-mm ID tubing, 18-cm long. These required cleaning by passing the cryogenically isolated CO_2 through PoraPlot Q packing material (Affek & Eiler, 2006; Davies & John, 2017). In our setup, a 4-mm ID borosilicate glass U tube was packed with PoraPlot Q (5 -mm ID, 7-cm length) and silver phosphate (entrance side, 1-cm length, mixed with quartz wool) and plugged with quartz wool then capped with silver wool. That was attached to the vacuum line, and the CO_2 was frozen over to another trap through the packing material at room temperature (transfer time ~45 to 50 min, determined empirically). The trap was baked out at 150 °C for 45+ min under vacuum between samples. Select samples were recleaned and reanalyzed, with the original analysis discarded if values shifted by >0.035 Δ_{47}.

The measurements on the mass spectrometer (MAT 253, Thermo) were made following the PBL protocol (interpolation) presented by He et al. (2012). The R-script from that work used to calculate Δ_{47} was modified to directly calculate $\delta^{13}C$ and $\delta^{18}O$, as outlined above for the model and running iterations until $X < 1 \times 10^{-9}$, later modified to use equations (10) and (11) with three iterations. It was also modified so different parameter sets could be used as noted, which cannot be done using the instrument's software. As presented in He et al. (2012), the PBL correction is not perfect and the residual baseline can be treated as a linear trend in Δ_{47} versus $^{47}\delta$. That correction was applied as noted to each set of runs for each parameter set used, as the slope would vary when the parameter sets were changed.

The data model was used to fit the EG results. The $\delta^{13}C_{VPDB}$ and $\delta^{18}O_{VSMOW}$ data from a series is used directly, the input parameter set can be varied, the output parameter set would be the one used to process the data, then the difference between the Δ_{47} model results and the Δ_{47} measured results can be minimized (sum of squares of differences) by varying PBL_{47}, Δ_{47} set value, and the parameter(s) of interest. This fitting does not directly account for expected noise in the data, and treats replicate runs independently of each other. The model baseline (PBL_{47}) scales to the m/z 44 input, in this case determined by the set value and the reported differences between the sample and WG. The residual PBL_{47} is expected to dominate Δ_{47} trends, and is fitted in lieu of m/z 47 linearity. Processing with different initial parameter sets in the model will give different Δ_{47} results relative to the working gas and different Δ_{47} versus $^{47}\delta$ trends.

2.3. Chemicals and Supplies

The CO_2 for the CO_2-water equilibration runs was supplied by OzTech Trading Corporation (OzTech, Safford, AZ) for use as CO_2 isotopic standards. Where stated, the water standards, VSMOW2 and SLAP (NIST, Gaithersburg, MD) were used as is. Older supplies, VSMOW, GISP, and SLAP, courtesy of Robert Clayton, were used after filtering through 0.2 micron syringe filters to remove visible contaminants. Other water used was either local water treated using a Nanopure system (Barnstead, Thermo), Chicago snow melt from 2012, or house RO (reverse osmosis) evaporatively enriched. The collected and evaporatively enriched

waters were treated with activated charcoal (Norit 3 mm, Spectrum) and filtered (0.22 micron nylon membrane, Tisch Scientific, North Bend, OH, using Millipore sintered glass support, EMD-Millipore, Darmstadt, German, or 0.22 micron Corning filtration unit, Corning, NY). The tube cracker was a section of flexible stainless steel tubing with Ultra-Torr fittings (Swagelok). The borosilicate glass tubing (Chemglass) was washed and ashed (500 °C overnight) before use. Other chemicals used were reagent grade or better.

3. Results

3.1. Model PBL and Δ_{17} Tests

He et al. (2012) showed that the PBL_{47} is a major contributor to the slope in the Δ_{47} vs $^{47}\delta$ plot of heated or equilibrated gases and estimated the PBL_{47} from the slope of that line. The results of our current model on a matrix of data for a −25 mV PBL_{47} effect on an approximate 2,500 mV *m/z* 47 signal are shown in Figure 1a, both with and without Δ_{47} versus $^{47}\delta$ slope correction. After the linear correction, the data points form a curve and are off by −0.019 at either end and by 0.007 at the middle, consistent with He et al. (2012)

The effect of generating the data with one parameter set, BAC, and processing with another, GSR, both with and without −25 mV PBL_{47}, is also shown (Figures 1b and 1c). The GSR processed points plotted against $^{47}\delta$ give a diamond shaped matrix (Figure 1b), not a line. The points will fall on a line if plotted against ($\delta^{13}C_{VPDB} - \delta^{18}O_{VSMOW}$; Figure 1d). Replotting GSR processed data against ($\delta^{13}C_{VPDB} - \delta^{18}O_{VSMOW}$) shifts the data points in the diamond pattern from $^{47}\delta$, which is approximately ($\delta^{13}C_{VPDB} + \delta^{18}O_{VSMOW}$), to ($\delta^{13}C_{VPDB} - \delta^{18}O_{VSMOW}$), which aligns the rows of constant $\delta^{18}O$ points in the data matrix, and the diamond pattern in $^{47}\delta$ space becomes the line seen in ($\delta^{13}C_{VPDB} - \delta^{18}O_{VSMOW}$) space (Figures 1b and 1d). In that way, the two types of plots present complementary information, akin to Δ_{47} versus $\delta^{13}C$ compared to Δ_{47} vs $\delta^{18}O$ plots. The ($\delta^{13}C_{VPDB} + \delta^{18}O_{VSMOW}$) and ($\delta^{13}C_{VPDB} - \delta^{18}O_{VSMOW}$) axes can be projected on a $\delta^{13}C$, $\delta^{18}O$ grid (supporting information, Figure S1, done assuming stochastic distribution of the isotopologues). To stay at 0 ($\delta^{13}C_{VPDB} - \delta^{18}O_{VSMOW}$), ($\delta^{13}C_{VPDB} + \delta^{18}O_{VSMOW}$) axis will have to fall on the $\delta^{13}C = \delta^{18}O$ line. By the same reasoning, ($\delta^{13}C_{VPDB} - \delta^{18}O_{VSMOW}$) axis falls on the $\delta^{13}C = -\delta^{18}O$ line, which is orthogonal to the $\delta^{13}C = \delta^{18}O$ line. The origin will shift with the WG, but the principle is the same. Correcting data in anyone of these four spaces will give a partial correction in the other three. For the best correction, use the axis that gives the best line, with a follow up correction done on the orthogonal axis.

The combined effects, PBL_{47} and GSR processing, give rise to a line when plotted against $^{47}\delta$, but a broad matrix of points if plotted against ($\delta^{13}C_{VPDB} - \delta^{18}O_{VSMOW}$; not shown but can be modeled using the model spreadsheet in the supporting information). After a Δ_{47} versus $^{47}\delta$ slope correction, plotting the data against $^{47}\delta$ shows the matrix pattern from the GSR processing combined with the curve of the data points due to PBL_{47} (Figure 1c). The endpoints of the diamond shaped matrix drop and the middle points rise (Figures 1b and c). Replotting the corrected data (Figure 1c) against ($\delta^{13}C_{VPDB} - \delta^{18}O_{VSMOW}$) shows a line, with a spread of data points, similar to the line from GSR processing data (no PBL_{47}) run, albeit with an offset, ~0.020 Δ_{47} (Figure 1d).

The model was used to examine effects of Δ_{17} on the Δ_{47}. Using the same parameter sets for generation and processing the data set, but varying the Δ_{17} shows that a 0.5‰ Δ_{17} shift relative to the reference gas leads to ~ −0.018 shift in Δ_{47} (Figure 1a), consistent with earlier work (Halevy et al., 2011). A 0.5‰ Δ_{17} shift also leads to a small shift in $\delta^{13}C$, ~0.035.

3.2. Modeling the Effects of Changes in Specific Parameters on Δ_{47} and $\delta^{13}C$

The accepted absolute ratios for the $\delta^{13}C$ and $\delta^{18}O$ standards have changed over time, as have the processing parameters used to related $\delta^{18}O$ to $\delta^{17}O$ (Table 1). Brand et al. (2010) noted that the $^{17}R/^{13}R$ relationship is robust, more so than ^{17}R and ^{13}R individually. To see the relative relationship of the different parameters to $^{17}R/^{13}R$, the ^{13}R, K, and λ values were varied in the BAC parameter set and those values were plotted against the corresponding part per thousand difference in $^{17}R_{VSMOW}/^{13}R_{VPDB}$ from the starting value, that is, $(^{17}R_{VSMOW}/^{13}R_{VPDB})_{BAC}$ (Figure 2a).

Changing ^{13}R, K, and λ also affected the model sample matrix. To study those effects, the difference between the nominal starting value and the modeled value, in both $\delta^{13}C$ and Δ_{47}, at the two extreme matrix points ($\delta^{13}C$, $\delta^{18}O$), (−50,50), and (0, 0), both ~0 $^{47}\delta$ but −100 and 0 ($\delta^{13}C - \delta^{18}O$) were subtracted from each

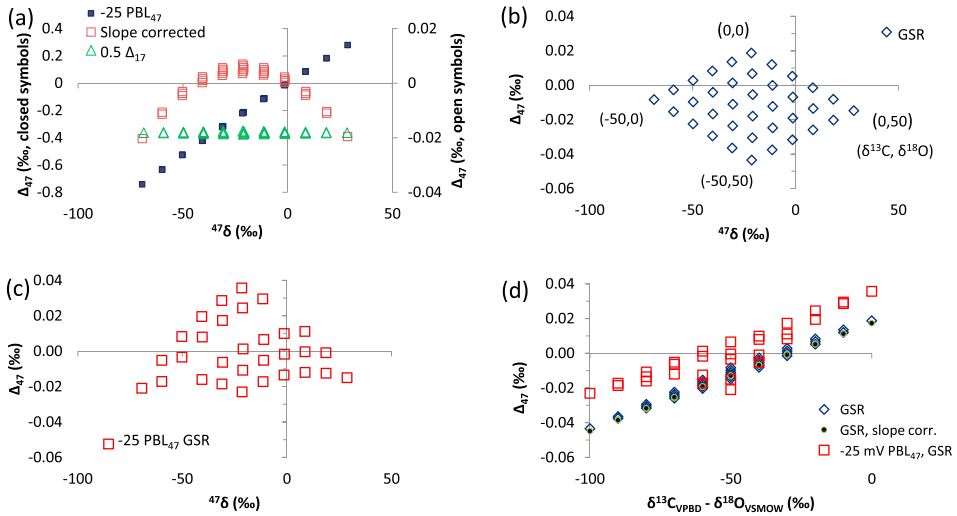

Figure 1. Effect of baseline and Δ_{17} on Δ_{47} values. Plots of Δ_{47} versus $^{47}\delta$ or ($\delta^{13}C_{VPDB} - \delta^{18}O_{VSMOW}$), as listed, for model data matrix: $\delta^{13}C$: −50 to 0; $\delta^{18}O$: 0 to 50; step size 10; reference gas −3.61 $\delta^{13}C$, 24.99 $\delta^{18}O$. Model data generated using BAC parameter set and processed with BAC set unless otherwise listed. Results plotted with and/or without Δ_{47} vs $^{47}\delta$ slope correction. (a) −25 mV PBL_{47}, 0‰ Δ_{17} (squares), both with slope correction (open) and without slope correction (closed). 0 mV PBL_{47}, 0.5‰ Δ_{17} with slope correction (open triangles) which overlaps uncorrected results (not shown). (b) 0 mV PBL_{47}, GSR parameter set (c) −25 mV PBL_{47}, GSR parameter set, slope corrected (20 $\delta^{18}O$ series not in matrix). (d) Replotting (b) and (c) results versus ($\delta^{13}C_{VPDB} - \delta^{18}O_{VSMOW}$) and including (b) series data with slope correction. Switching to ($\delta^{13}C_{VPDB} - \delta^{18}O_{VSMOW}$) scale moves the data points horizontally.

other, giving a measure of scale compression along the ($\delta^{13}C - \delta^{18}O$) axis. The difference of differences, $\delta^{13}C_{diff}$ and $\Delta_{47\ diff}$, is plotted against $(^{17}R_{VSMOW}/^{13}R_{VPDB})_{BAC}$. The effect on $\delta^{13}C_{diff}$ is about twice that seen for $\Delta_{47\ diff}$, and in opposite directions (Figure 2b). Daëron et al. (2016) also reported that relative per mil effects on $\delta^{13}C$ were twice the effects seen on Δ_{47} when ^{17}O was varied. Varying the different components gave rise to different matrix shapes (not shown). That is, the effects are not identical, which is reflected in the $\delta^{13}C_{diff}$ or $\Delta_{47\ diff}$ versus $(^{17}R_{VSMOW}/^{13}R_{VPDB})_{BAC}$ slopes that vary slightly for the different components.

The different parameter sets can vary in more than one parameter, as shown in Table 1, and the combined effect on either $\Delta_{47\ diff}$ or $\delta^{13}C_{diff}$ as a function of the net change in $(^{17}R_{VSMOW}/^{13}R_{VPDB})_{BAC}$ space is also shown in Figure 2b. The A&B set is very close to the BAC set in $(^{17}R_{VSMOW}/^{13}R_{VPDB})_{BAC}$ and shows little change in $\Delta_{47\ diff}$ or $\delta^{13}C_{diff}$. The $^{13}R_{VPDB}$ difference counteracts the effect from the $^{17}R_{VSMOW}$ difference,

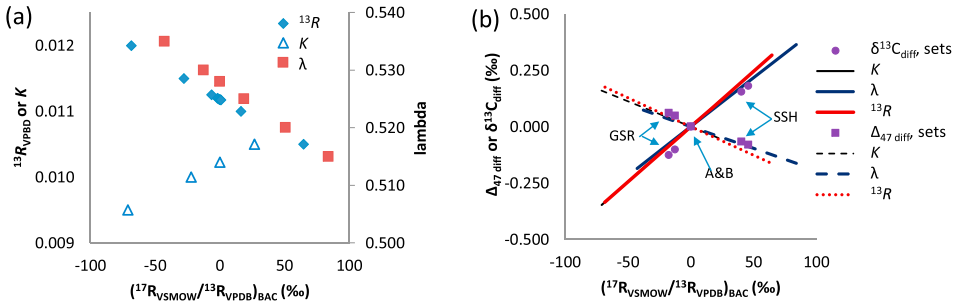

Figure 2. Modeling parameter sets and components in $(^{17}R_{VSMOW}/^{13}R_{VPDB})_{BAC}$ space (see Table 1). (a) Components, $^{13}R_{VPDB}$, K, or λ, in BAC parameter set individually varied over range of values reported (Table 1) and plotted against corresponding $(^{17}R_{VSMOW}/^{13}R_{VPDB})_{BAC}$ value. (b) Scale compression along ($\delta^{13}C$-$\delta^{18}O$) axis, the difference of the differences between the expected and modeled results at (50, −50) and (0,0) matrix data points ($\delta^{13}C$, $\delta^{18}O$) for $\delta^{13}C$, ($\delta^{13}C_{diff}$) or Δ_{47} ($\Delta_{47\ diff}$) plotted against $(^{17}R_{VSMOW}/^{13}R_{VPDB})_{BAC}$. Matrix data generated with $\Delta_{47,WG} = 0.9$ and $\Delta_{47,\ sample} = 0.4$ using BAC parameter set, then processed with modified BAC parameter set, individual component values varied as above, or with other parameter sets: SSH, SSH using the updated value for $^{13}R_{VPDB}$ (not in Table 1), GSR, GSR set with the updated value for $^{13}R_{VPDB}$, (not in Table 1) and A&B.

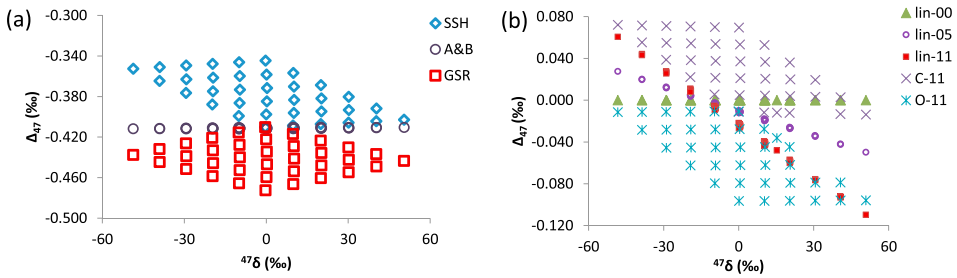

Figure 3. Modeling effects seen by shifting parameter sets or linearity. Model, BAC parameter for sample generation, vary processing parameters, 0 mV PBL_{47}, $\delta^{13}C$: −50 to 0; $\delta^{18}O$: 0 to 50; reference gas −0 $\delta^{13}C$, 0 $\delta^{18}O$. Generated Δ_{47} plotted against $^{47}\delta$, uncorrected. (a) Processing parameter sets, GSR, SSH or A&B; working gas at 0.9 Δ_{47}, samples set to 0.5 Δ_{47}. (b) Processing parameter set BAC, linearity settings (‰/V ^{45}R, ‰/V ^{46}R): lin-00 (0.00, 0.00); lin-05 (0.05, 0.05); lin-11 (0.11, 0.11); C-11 (0.11, 0.00); and O-11(0.00, 0.11). Amplitude offset between working gas and samples: 0.1 V. Nominal signal strength 16 V. Working and sample gas Δ_{47} values the same: 0. Intercepts of lin-05 and lin-11 fitted lines are at −0.010 and −0.022 Δ_{47} respectively.

for example, $\Delta_{47\ diff} = 0.002$, but is 0.012 if only the ^{17}O components from the A&B are used, that is, only K is changed (Table 1). The other parameter sets do differ in $(^{17}R_{VSMOW}/^{13}R_{VPDB})_{BAC}$, with the GSR set at −17.6 and SSH at +40.4. Both of these sets sit above the other data lines and the net difference in $\Delta_{47\ diff}$ space have close to the same magnitude, ~0.063 $\Delta_{47\ diff}$, though opposite in sign (Figure 2b).

The effect of switching parameter sets on the full matrix is seen by plotting Δ_{47} versus $^{47}\delta$, Figure 3a, with the spread in the data points at 0 $^{47}\delta$ corresponding to the data plotted in Figure 2b. The data were generated using the BAC set with 0.9 Δ_{47} WG and 0.5 Δ_{47} samples, a 0.4 difference. The calculated Δ_{47} using the same parameter set, BAC, is −0.410. A slight difference due to data processing assuming stochastic distribution leading to scale expansion in Δ_{47}. The A&B parameter set is also ~−0.410, with little spread in the data points. The SSH parameter set expands the matrix to higher values and GSR to lower values. The shape of the matrix varies from diamond to rhomboid. If the Δ_{47} data are plotted against $(\delta^{13}C_{VPDB} - \delta^{18}O_{VSMOW})$, the GSR results, diamond shaped, collapse onto a line, as shown in Figures 1b and 1d under slightly different conditions. The SSH results shift but do not collapse down onto a line, unless a Δ_{47} versus $^{47}\delta$ correction is applied (not shown).

3.3. Modeling Linearity Effects on Δ_{47}

Linearity issues on ^{45}R and ^{46}R can affect the $\delta^{13}C$ and $\delta^{18}O$ results, which affects the calculated expected $^{47}\delta$ and thus the Δ_{47} values. Values of 0.050‰ and 0.110‰/V were applied to ^{45}R and/or ^{46}R, with a 0.1 V (100 mV in model) offset from WG, 16 V on m/z 44. The results are shown in Figure 3b. If the linearity is the same for ^{45}R and ^{46}R, a line is seen in Δ_{47} versus $^{47}\delta$. That is correctable, as long as the sample amplitudes (mV) are the same. The net offset in Δ_{47} is due to the millivolt offset between samples and standards. If the linearity is only applied to one mass at a time, then plotting Δ_{47} versus $^{47}\delta$ shows a spread of data that resembles what is shown in Figure 3a. Linearity effects mimic effects seen when parameter sets are switched in the model. Data generated using the BAC parameter set with 0.04‰ and −0.04‰/V on ^{45}R and ^{46}R are best processed by using the GSR parameter set, after Δ_{47} versus $^{47}\delta$ correction, run at 16-V setting. The SSH parameter set works best after Δ_{47} versus $^{47}\delta$ correction if the linearity values are set to −0.04‰ and 0.05‰/V, respectively. The linearity effect scales with target voltage used in the model. If the voltage is varied among samples, results will vary too and add apparent noise to the results (see spreadsheet model in supporting information).

The linearity effects on Δ_{47} can also be mimicked by changing other parameters, for example, a 0.05‰/V linearity on either ^{45}R or ^{46}R could also be mimicked by adjusting the respective PBL value to 14 mV PBL_{45} or 17 mV PBL_{46}. It is not a perfect match. The linearity effect will vary with m/z 44 offsets between the sample and WG settings, but the PBL values scale with m/z 44, so its effect is about the same. These PBL values are much larger than typically measured on the instrument.

The linearity on m/z 44, in this case the change in intensity with pressure modeled as mV differences on m/z 44, can also be tested in the model. A 0.1‰/V change in m/z 44 will give rise to an apparent −0.1‰/V shifts in ^{45}R and ^{46}R with changes in m/z 44 amplitude. Linearity is determined experimentally by changing gas

pressure, modeled as changing m/z 44. This value will be the net value in the model, that is the ^{45}R, ^{46}R, or ^{47}R set linearity values minus the m/z 44 value. The linearity effect breaks down into two parts. The set values govern how the system responds to amplitude differences on a given m/z due to isotopic differences, that is the effect on the different points in the model matrix. The experimentally determined or net value governs how the WG responds to changes in m/z 44 amplitude. When modeling experimental results, m/z 44 value will be added to the other values to maintain a constant net value, which is the apparent linearity, that is, the value determined when pressures are changed. If all linearity values are the same, for example, 1‰/V, the net will be zero, as would be the experimentally determined value, but there would be scale expansion for $\delta^{13}C$ and $\delta^{18}O$, ~0.8 at 50‰ run at 16 V m/z 44, though only 0.021 Δ_{47} change at −50 $\delta^{13}C$, 50 $\delta^{18}O$.

3.4. Modeling Other Effects on Δ_{47}

If the two main isotopologues that compose a given m/z value have different absolute abundances,an FI effect, that can resemble linearity effects. As modeled, the FI variable is just a multiplier on the main ^{17}O containing isotopologue, which is the second most abundant isotopologue at a given m/z. For example, with m/z 45, if $^{16}O^{12}C^{17}O$ is 0.5% less in terms of absolute abundance than $^{16}O^{13}C^{16}O$, $FI_{45} = 0.995$. The differences in FI will not show up in a traditional measurement of linearity since it is just scaling a component of the signal. The Δ_{17} component is similar to FI, except it affects all ^{17}O isotopologues, not just the designated one.

The FI feature can be used to examine the different minor isotopologue excesses calculated by Wang et al. (2004), equation (9), though that would only have a minor effect on the Δ_{47} results, <0.002.

3.5. The Effects of Different Parameter Sets on Equilibrated Gas Runs

Running samples having the same $^{47}\delta$ and Δ_{47}, but large spreads in $\delta^{13}C$ and $\delta^{18}O$ will help highlight the differences between using different parameter sets for data processing. This is seen in Figures 3a and 3b, where a vertical row at a given $^{47}\delta$ shows Δ_{47} shifting with changes to $\delta^{13}C$ and $\delta^{18}O$. To do that in the laboratory, two CO_2 gases with a spread in $\delta^{13}C$ values (nominal values ~−40 and −10 $\delta^{13}C_{VPDB}$) were equilibrated with at least three different waters, house waters at −23, 1.5, and 30 $\delta^{18}O_{VSMOW}$ (equilibrated gas 1, EG1, Figures 4a and 4b) or VSMOW2 and SLAP plus a 50:50 mix of those standards (EG2, Figures 4c and 4d). A follow up run was also done, with the CO_2 gases equilibrated with house enriched water and with older samples of VSMOW, GISP, and SLAP (EG3, Figures 5 and 6). The samples were equilibrated at 26 °C so they would all have the same Δ_{47}, with any differences in the measurements due to handling, uncorrected PBL, missed or miss applied corrections, or errors in the parameters used to process the data. The different EG sets were run at different times and under different mass spectrometer conditions. The same tank of CO_2 gas, −3.61 $\delta^{13}C_{VPDB}$ and 24.99 $\delta^{18}O_{VSMOW}$, was used as the working reference gas in all cases.

The first test, EG1, modeled with the BAC parameter set, or BAC model, works better than the GSR model. There is less spread between the different samples that run near the same $^{47}\delta$ value (Figure 4a). Also note, using the different parameter sets will not lower the scatter in replicate runs. These results are consistent with previous studies (Daëron et al., 2016; Schauer et al., 2016). When the GSR model in used, a linear trend in ($\delta^{13}C_{VPBD} - \delta^{18}O_{VSMOW}$) is seen (Figure 4b). The measured linearity for both ^{45}R and ^{46}R was 0.011‰/V.

EG2, with a limited number of samples and analyzed under different mass spectrometer conditions, did not give the same results (Figures 4c and 4d). The GSR model shows less scatter than the BAC model. Plotting the Δ_{47} results against ($\delta^{13}C_{VPDB} - \delta^{18}O_{VSMOW}$) shows a stronger correlation when using the BAC model than the GSR model (Figure 4d), implying the GSR model is the better choice. The linearity was 0.011‰ and 0.056‰/V for ^{45}R and ^{46}R, respectively.

EG3 analyzed a suite of samples with the same or replicate gas samples analyzed at different gas pressures with the same tune settings, EG3a at 16 V on m/z 44 and EG3b at 12 V on m/z 44, as well as under different tune settings, EG3c 12 V on m/z 44. The linearity values for EG3a were initially 0.024‰ ± 0.010‰ and 0.036‰ ± 0.019‰/V for ^{45}R and ^{46}R when measured over a range of 14.5 to 16.5 V on m/z 44, 0.5-V increments. After a week, the values were 0.035‰ and 0.044‰/V, respectively. If the measurement range was shifted to 13 to 16 V, the linearity values shifted to 0.021‰ ± 0.007‰ and 0.074‰ ± 0.011‰/V, respectively. For EG3b, over the 11 to 13-V range, the values were 0.049‰ and 0.095‰/V for ^{45}R and ^{46}R. The linearity for the alternate tune setting was 0.022‰ and 0.049‰/V for ^{45}R and ^{46}R over the 11- to 13-V range for those 12-V runs.

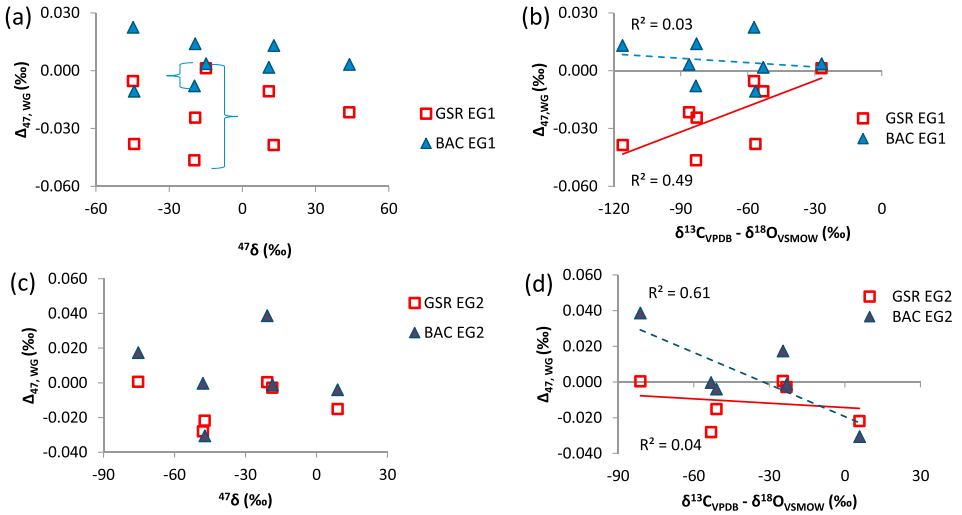

Figure 4. Equilibrated gases (EG) studies. All data pressure baseline corrected, processed with different parameter sets, BAC or GSR, Δ_{47} versus $^{47}\delta$ slope corrected, with trend lines, BAC (solid) and GSR (dashed). (a) Plot of Δ_{47} versus $^{47}\delta$ for EG1, 26 °C, house waters, −0.011‰/V linearity (uncorrected) on both ^{45}R and ^{46}R, with reruns data at −10,17; −10, 43, and −41, 17 (δ^{13}C, δ^{18}O). The brackets indicate the differences between two samples, at −20 $^{47}\delta$ but with different δ^{13}C and δ^{18}O values, processed with either the GSR or BAC parameter set. (b) Replot of EG1 Δ_{47} data versus ($\delta^{13}C_{VPDB} - \delta^{18}O_{VSMOW}$). (c) Plot of Δ_{47} versus $^{47}\delta$ for EG2, 26 °C, VSMOW2, mixture and VSLAP, −0.011‰/V ^{45}R and −0.056‰/V ^{46}R (uncorrected). Samples having large differences in δ^{13}C and δ^{18}O but same $^{47}\delta$ fall in −20 and −48 $^{47}\delta$ regions. (d) Replot of EG2 Δ_{47} data versus ($\delta^{13}C_{VPDB} - \delta^{18}O_{VSMOW}$).

Concentrating on EG3a and plotting the Δ_{47} results against ($\delta^{13}C_{VPDB} - \delta^{18}O_{VSMOW}$) does not show a strong correlation with either parameter set (Figures 5a and 5b). A trend with a few outliers does emerge when plotting Δ_{47} versus average difference in amplitude between sample and reference gases, especially when using the BAC model (Figure 5c). Two of the three apparent outliers were duplicate analyses of the same sample gas. Further analyses were then done comparing measured results to the model system.

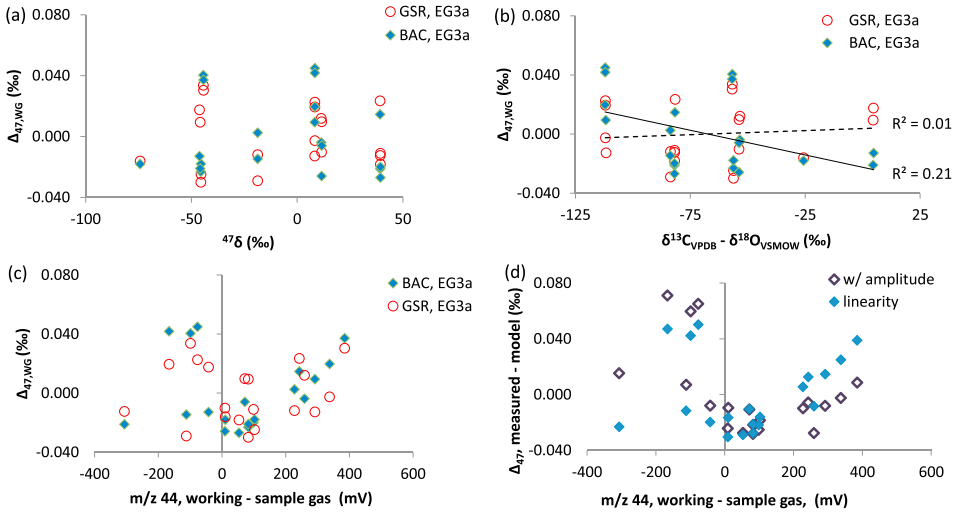

Figure 5. Equilibrated gas studies, amplitude effects. Plot of equilibrated gases results, EG3a, run at 16 V m/z 44 nominal amplitude, 0.024‰/V ^{45}R and 0.036‰/V ^{46}R linearity. Data processed using pressure baseline correction with designated parameter set and a Δ_{47} versus $^{47}\delta$ correction applied. Corrected Δ_{47} results plotted against: (a) $^{47}\delta$, (b) ($\delta^{13}C_{VPDB} - \delta^{18}O_{VSMOW}$) with trend lines shown, solid for BAC and dashed for GSR data sets and (c) plotted against average difference in m/z 44 amplitude between WG and sample, working − sample gas. Two of the three apparent outliers in (c), near 0.040, −100 for BAC processed results, are reruns of the same gas. (d) Corrected Δ_{47} results processed with BAC parameter set and linearity correction.

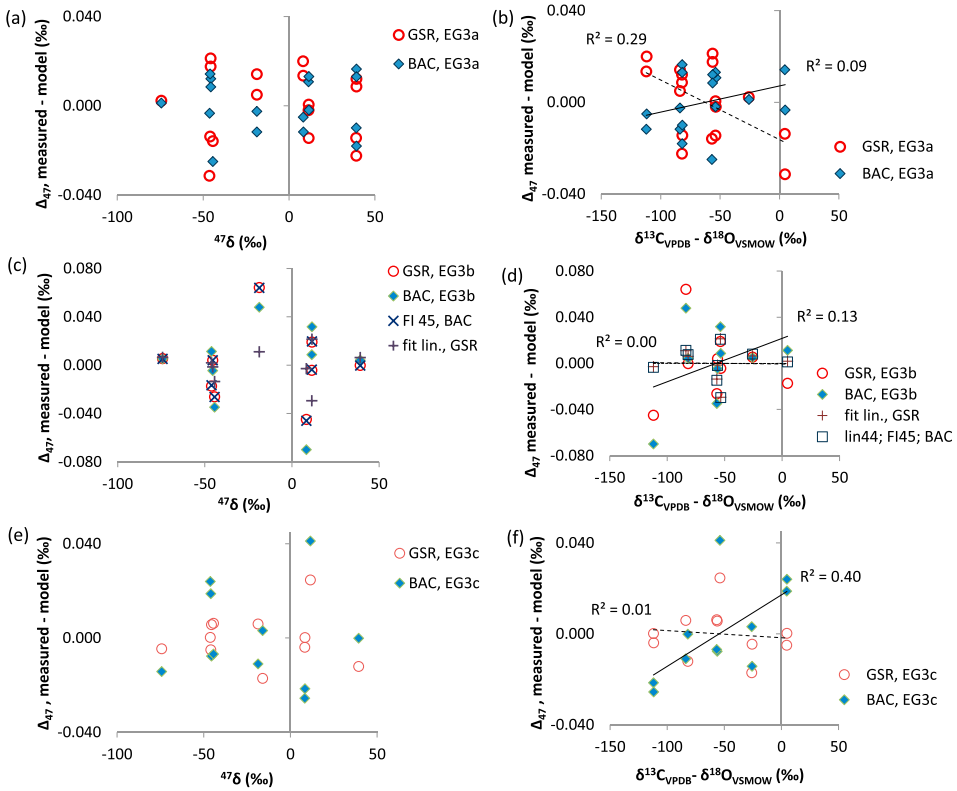

Figure 6. Equilibrated gas series three, EG3, comparing different tune settings. Measured minus modeled results plotted against $^{47}\delta$ or ($\delta^{13}C_{VPDB} - \delta^{18}O_{VSMOW}$), with trend lines (linear) and correlation coefficients squared shown in the latter case. The model data were generated using either the BAC or GSR parameter sets and corrected using the reported linearity and amplitude differences between sample and working gas. Other parameters fitted as noted. Trend lines, when shown, solid for BAC and dashed for GSR. (a) EG3a tune setting, 16V amplitude, data points with outliers excluded, plotted against $^{47}\delta$ and (b) plotted against ($\delta^{13}C_{VPDB} - \delta^{18}O_{VSMOW}$). (c) EG3b, using EG3a tune settings but run at 12 V amplitude, data points plotted against $^{47}\delta$ and (d) ($\delta^{13}C_{VPDB} - \delta^{18}O_{VSMOW}$). Also shown for EG3b are difference from the model system that includes fitting to FI on m/z 45 (FI 45, BAC), fitting to ^{45}R and ^{46}R linearity instead of keeping them fixed (fit lin.), and fitting to m/z 44 linearity and FI_{45} while keeping the ^{45}R and ^{46}R linearity fixed (lin44-fix45,46; FI45; BAC). (e) EG3c tune setting run at 12V amplitude and plotted against $^{47}\delta$ and (f) ($\delta^{13}C_{VPDB} - \delta^{18}O_{VSMOW}$).

3.6. Using the Model to Help Interpret Data

In EG3a, the differences in amplitude between the reference and sample gases was affecting the results (Figure 5c). The EG3a data were then put into the model and the various settings tested to see how that setting might be affecting the results. The differences between the model and sample data are plotted against m/z 44 amplitude difference (working reference and sample gas) after applying ^{45}R and ^{46}R linearity and amplitude corrections (Figure 5d). The three apparent outliers seen in Figures 5c and 5d at ~−100 mV and 0.040 Δ_{47} are only outliers when using the BAC model, determined by using Peirce's test (Ross, 2003). One of the outlier samples, at −44.3 $^{47}\delta$, Figure 5a, was recleaned and reanalyzed, and a difference between their Δ_{47} values was observed after linearity corrections were applied. The others, replicate runs at 8.4 $^{47}\delta$, were 0.020 to 0.030 Δ_{47} greater than the replicate analyses on a replicate sample before linearity corrections. If the GSR model was used in the model, the Δ_{47} values may shift but the differences between the replicate runs hold. However, none of the data points qualify as an actual outlier.

The data from each EG3 series were compared to the model data after corrections for linearity, on ^{45}R and ^{46}R, and amplitude, m/z 44, differences (Figure 6). The corrected EG3a series, with the outliers removed, now shows less scatter with the BAC model than the GSR model, and the GSR model shows a small correlation of Δ_{47} with ($\delta^{13}C_{VPDB} - \delta^{18}O_{VSMOW}$; Figures 6a and 6b), reversing the results without the corrections (Figure 5b). If FI_{45} is included in the fitting of the model to the samples, both parameter sets converge onto the same Δ_{47} values, within 0.010 Δ_{47} of the BAC model (not shown).

The EG3b series, run under the same tune settings but at a target intensity of 12 V on m/z 44, not 16 V, does not appear to favor either the GSR or the BAC models (Figures 6c and 6d). Both show a lot of scatter and little correlation of Δ_{47} with ($\delta^{13}C_{VPDB} - \delta^{18}O_{VSMOW}$), and this is after linearity corrections were applied. Different outliers were detected using the BAC and GSR models, the lowest data point with BAC and the highest one with GSR, as plotted (Figure 6c). The BAC model outlier sample corresponds to one of the outlier samples seen in EG3a. The GSR model outlier does not.

There is a lot of scatter in the results of the EG3b series, regardless of the parameter set used. The standard deviation for the Δ_{47} values, all points, is 0.035, BAC model, or 0.031, GSR model. If FI_{45} fitting is included, the data points in both models will overlap the GSR model results (Figure 6c, GSR, BAC, and FI45 plots). Removing the outlier appropriate for the given parameter set drops the standard deviations down to 0.020 and 0.023, respectively.

Fitting the linearity values, instead of using the measured ones, improved the fit. The fitted values were −0.056‰ and −0.035‰/V for ^{45}R and ^{46}R, respectively, when using the GSR model (Figure 6b, "fit lin, GSR"). The reported values were 0.021‰ to 0.049‰ and 0.071‰ to 0.095‰/V. A 0.1‰/V difference between the fitted and reported values indicates there are undetected problems.

The reported values can be used, 0.046‰ and 0.095‰/V for ^{45}R and ^{46}R, respectively, and the linearity on m/z 44 fitted. The points from that fit overlap the points from the fit to ^{45}R and ^{46}R linearity (Figure 6d, fit lin, GSR and "lin44; FI45, BAC"). As plotted, the fit to the linearity on m/z 44 used the BAC model and included fitting to FI_{45}, equivalent to using the GSR model in this series. With this fit, the standard deviation dropped to 0.015 without removing outliers. The fitted value was −0.234‰/V for linearity on m/z 44. Excluding the outliers from the fitting routine did not greatly improve the standard deviation, 0.014, of the remaining data points, but did shift the fitted value to −0.071‰/V. The changes in the linearity on m/z 44 were added onto the values for ^{45}R and ^{46}R to keep those values constant in terms of how the actual measurements are made.

If all the samples that were detected as outliers, in either EG3a or EG3b series, three points total, were removed from this analysis, then the modeled ^{45}R and ^{46}R linearity values, 0.078‰ and 0.077‰/V respectively, would partially overlap the range of reported values. That could not be done using the information from just this series. Fitting to the linearity on m/z 44 then either happened to fit the outliers well or those points are not actual outliers in this series.

Moving to different tune settings at 12 V intensity, EG3c, favors the GSR model. Less scatter is seen with the GSR model and there is a correlation of Δ_{47} with ($\delta^{13}C_{VPDB} - \delta^{18}O_{VSMOW}$) with the BAC model (Figures 6e and 6f). Additional fitting of the m/z 44 linearity only had minor effects, 0.002 Δ_{47} differences. Fitting to FI_{45} too had little effect on the GSR model, but the BAC results collapsed onto the GSR results (0.988 FI_{45}, plot not shown, linearity corrections on ^{45}R and ^{46}R included). Fitting to PBL_{45} with the BAC model gave very similar results to fitting to FI_{45}. The fitted value, −17 mV PBL_{45}, though, is outside the expected value for the residual PBL_{45}, ca. 1 mV, estimated from high voltage scans across m/z 45 peak.

The same fitting exercises can be done with FI_{46}, FI_{47}, PBL_{46}, Δ_{17}, and ^{45}R and ^{46}R linearity with similar results. Fitting to the ^{45}R and ^{46}R linearity instead of FI_{45}, using the BAC model, gives values that are significantly different than the reported values, by 0.04‰ and −0.07‰/V, respectively. The error in the reported linearity values ranged from 0.01‰ to 0.02‰/V. The model can be used to fit the other variables, though that may not be appropriate nor the results reasonable, for example, fitted result of −24 Δ_{17} (samples) is well outside the expected range for the surface of the Earth (Luz & Barkan, 2010).

Fitting a single subset of variables will partially correct for all problems in a data set, including errors in other variables and sample noise. That can lead to some interesting results, as shown above. In the EG3 series, FI_{45} has served as the catchall variable that will get the BAC and GSR model values to overlap. If the isotopologues do have different absolute abundances, then FI_{46} and FI_{47} need to be considered. Fitting to two or all three FI components at the same time will push the values past their individually fitted values, though the sample results stayed basically the same. The interactions between the different variables and the fitting routine will not always be useful. Two FI variables can be set and the third fitted to bring all three into the 0.99 to 1.01 range and get essentially the same sample results in the EG3c set as fitting only to FI_{45}. In this case, the model does not provide an exact solution but does allow for an exploration of what is possible.

4. Discussion

The clumped isotope community is aware of the practical issues in making their measurements (Dennis et al., 2011; He et al., 2012; Huntington et al., 2009). This model system highlights the effects those and other issues have on the clumped isotope measurements, as well as how they interact with each other. The matrix of data points plotted in Figures 1 and 3 shows how linearity issues, different parameter sets, Δ_{17}, and PBL_{47} shift and distort the Δ_{47} results. These can combine to mimic or mask each other. The different parameter sets, and the components that make them up, for example, *K*, show a linear relationship when plotting their effects on scale compression against $(^{17}R_{VSMOW}/^{13}R_{VPDB})_{BAC}$ (Figure 2b). FI_{45} is one of the variables modified when fitting EG data. Mathematically, FI_{45} serves as a multiplier for *K* in equation (4) (Table A1 line 14 traced back to line 4), at least for *m/z* 45. Modifying *K* moves the working parameter set along the $(^{17}R_{VSMOW}/^{13}R_{VPDB})_{BAC}$ line, Figure 2a, and empirically fits the parameter set to the EG data points (Figure 2b). That is how the fitted results processed with the BAC parameter set can fall on top of the GSR results (Figure 6c, "FI 45, BAC").

Modeling the linearity effect, ^{45}R and ^{46}R, shows that even at values typically considered acceptable, Δ_{47} results will be affected. As modeled, a linearity of 0.040‰/V for ^{45}R and −0.040‰/V for ^{46}R would shift results generated using the BAC parameter set to ones best processed by the GSR parameter set. This is demonstrated in EG studies. EG1 series works best with the BAC parameter set, consistent with the earlier papers (Daëron et al., 2016; Schauer et al., 2016). However, a short test, EG2, under different tune conditions that had larger (magnitude) linearity on ^{45}R and ^{46}R worked best with the GSR parameter set.

Correcting for linearity issues can help, as shown in the EG3a study. But that only worked well after outliers were removed, and the outliers were only detected when the BAC parameter set was used (Figures 5c and 5d and 6a and 6b). In the EG3b series, one of the samples was flagged as an outlier when processed with the BAC parameter set (Figures 6c and 6d, the low point), and a completely different sample was flagged when the GSR set was used (Figures 6c and 6d, the high point). The choice of processing parameters will not only affect your results, it can affect what data you choose to include in your results. The best practice would be to have multiple replicates of every data point, if feasible, and use those results to find outliers.

The choice of parameter set may not be obvious, as in EG3b, or the GSR set may be favored, as in EG3c, even after linearity corrections (Figure 6). Fitting to FI_{45} will cause the results converge on the GSR parameter set results when starting with either the GSR or BAC parameter sets, as shown in Figure 6c for the BAC parameter set. The EG3a series gave similar results, but in that case the results converged on values closer to the BAC parameter set results (not plotted). Fitting to FI_{45} is empirically fitting the parameter sets to the data along the *K* trajectory. If that is needed, it could indicate missing or improper corrections, poor quality data, or, indeed, the FI effect is real or source scrambling is affecting results.

The fitted values for FI_{45} are ~0.99, that is the absolute abundance of the ^{17}O isotopologues at *m/z* 45 is 99% of that for the ^{13}C isotopologue. Westley et al. (2007) report relative percent level differences between isotopologues for the generation of NO from N_2O in the mass spectrometer source. Though not CO_2, it did show source conditions affecting relative isotopologue abundances. Our results are evidence for, though not proof of, isotopologue absolute abundance differences in CO_2 mass spectrometry. Fitting to FI can also correct for other issues and allows for empirically fitting the parameter set to the data, limiting the utility of these results in understanding CO_2 source chemistry.

The EG3b results also showed that fitting to *m/z* 44 linearity helped minimize the scatter in the samples. However, one cannot distinguish between possible outliers driving the *m/z* 44 linearity fit, fitting to noise/outliers, or that the apparent outliers are due to an unaccounted for linearity effect on *m/z* 44 under these conditions. If sample information is used from the EG3a series, then more outliers can be removed and the impact of fitting to *m/z* 44 linearity diminishes. Fitting to it only had a minor effect when tested on the other trials. The modeling shows that linearity can be broken into two components, and linearity of *m/z* 44 can be determined indirectly as $\delta^{13}C$ and $\delta^{18}O$ scale compression that is not in line with ^{45}R and ^{46}R linearity.

It is also important that the sample and WG are run at the same signal strength. That will limit the impact of linearity issues. However, if samples are analyzed over a wide range of pressures, then linearity measurements and corrections would have to be made accordingly. Long-integration dual inlet protocols (Hu

et al., 2014; Müller et al., 2017) fall into that category. Long integration times can mean the sample gas will bleed down over a wide range of voltages. Linearity has to be consistent, and small, over that entire range. If it varies, then either a running correction or an appropriate correction to a weighted average would have to be made. As seen here with EG3a and EG3b, samples with the same tune settings but run at different voltages, 16 and 12 V on *m/z* 44, behave differently. If different samples are run over different voltage ranges, no matter the protocol, they could need their own suite of standards, empirical transfer functions, PBL corrections, etc.

Though not presented here, the model can be used to see how linearity, choice of parameter set used for processing, etc., affects interlaboratory studies. Any three points in the data matrix can be picked to be "standards" and two or more for samples. The interplay between them can be mapped out as conditions change, and that represents how values can vary between instruments or sessions with different instrument tunings. This can also be done with available working standards (Bernasconi et al., 2018).

The solution for solving equation (3) presented here, equations (10) and (11), works well. The approximations used for calculating the isotopes in Brand et al. (2010) will lead to deviations from the exact solution, as they pointed out, which might lead to Δ_{45} and Δ_{46} artifacts and the need to use full Δ_{47} if incorporated into clumped isotope studies. Other methods work, for example, Taylor expansion (Daëron et al., 2016), and all methods can be evaluated using equation (3).

5. Conclusions

We see that getting the correct stable isotope results for CO_2 requires more than just choosing the most recent, BAC, parameter set for the needed ^{17}O correction. We have demonstrated that the apparent proper parameter set can vary with the tuning used and the instrument's linearity, which could skew both inter and intralaboratory corrections and results. This will add to the apparent noise seen in sample data and is likely contributing to the precision seen in the analysis of previous work (Fernandez et al., 2017).

Modeling the data, as done here, can lead to insights into issues affecting the quality of the data. It is not just that ^{45}R and ^{46}R linearity can affect results, and corrections do need to be applied, but it is that other factors can also affect results. A model, such as this, can be used as a tool to evaluate data, for example, ETF data. It should not be used for data correction but can point toward over looked problems that need to be addressed and/or standards that need to be run.

We recommend the following:

1. Mass spectrometer data can and should be directly processed for $\delta^{13}C$, $\delta^{18}O$, and Δ_{47} determination using the method presented here or any suitable method that is checked against equation (3). That way corrections can be applied to the data prior to processing.
2. Linearity corrections, ^{45}R, ^{46}R, and including *m/z* 44 if scale compression is an issue, should be done. Most importantly, tune the instrument well to avoid needing to do such corrections.
3. Use a model system, such as the one presented here, to test the effects the measured linearity would have on your suite of standards and samples.
4. Laboratories should use the currently accepted values for the parameters for $^{13}R_{VPBD}$ and ^{17}O determination (Brand et al., 2010; Coplen et al., 2002; Daëron et al., 2016; Schauer et al., 2016).
5. Results should be presented in the ARF (Dennis et al., 2011). Though not discussed in detail here, that can also be done by correcting samples to a suite of standards (Bernasconi et al., 2018).
6. Plot Δ_{47} values from standards, EGs and HGs against ($\delta^{13}C - \delta^{18}O$), after Δ_{47} versus δ_{47} correction. Trends indicate incomplete linearity corrections or issues with the source, for example, FI_{45}.

Appendix A: Tables

This appendix contains two tables for showing the equations used in the model. Table A1 shows how the model data are generated. Table A2 shows how the model data are processed to give isotopic results.

Table A1
Model Data: Fractional Amounts for 44, 45, 46, and 47 From Parameter Set (Table 1) and Initial $\delta^{13}C$, $\delta^{18}O$, and Δ_{47} Input

Species	Working gas (reference)	Sample
1. 13	$^{13}R_{WG} = {}^{13}R_{VPDB} \times (1 + (WG\ \delta^{13}C + \delta^{13}C_{offset})/1000)$	$^{13}R = {}^{13}R_{VPDB} \times (1 + \delta^{13}C)/1000$
2. 12F	$^{12}F = 1/(1 + {}^{13}R)$	
3. 18	$^{18}R_{WG} = {}^{18}R_{VSMOW} \times (1 + (WG\ \delta^{18}O + \delta^{18}O_{offset})/1000)$	$^{18}R = {}^{13}R_{VSMOW} \times (1 + \delta^{18}O)/1000$
4. 17	$^{17}R = K \times {}^{18}R^{\lambda} \times (1 + \Delta_{17}/1000)$	
5. 16F	$^{16}F = 1/(1 + {}^{17}R + {}^{18}R)$	
6. 13F	$^{13}F = {}^{12}F \times {}^{13}R$	
7. 18F	$^{18}F = {}^{16}F \times {}^{18}R$	
8. 17F	$^{17}F = {}^{16}F \times {}^{17}R$	
9. 47F′	$^{47}F^{\dagger} = 2 \times {}^{13}F \times {}^{18}F \times {}^{16}F + 2 \times {}^{12}F \times {}^{18}F \times {}^{17}F + {}^{13}F \times {}^{17}F^2$	
10. 44F	$^{44}F = {}^{12}F \times {}^{16}F^2$	
11. 13F′	$^{13}F' = {}^{13}F - {}^{47}F^{\dagger} \times \Delta_{47}/1000$	
12. 16F′	$^{16}F' = {}^{16}F' - {}^{47}F^{\dagger} \times \Delta_{47}/1000$	
13. 18F′	$^{18}F' = {}^{18}F' - {}^{47}F^{\dagger} \times \Delta_{47}/1000$	
14. 45F	$^{45}F = {}^{13}F' \times {}^{16}F'^2 + 2 \times {}^{12}F \times {}^{16}F' \times {}^{17}F \times FI_{45}$	
15. 46F	$^{46}F = 2 \times {}^{12}F \times {}^{18}F' \times {}^{16}F' + 2\ x\ {}^{13}F' \times {}^{16}F' \times {}^{17}F \times FI_{46} + {}^{12}F \times {}^{17}F^2$	
16. 47F	$^{47}F = (2 \times {}^{13}F \times {}^{18}F \times {}^{16}F + 2 \times {}^{12}F \times {}^{18}F \times {}^{17}F \times FI_{47} + {}^{13}F \times {}^{17}F^2) \times (1 + \Delta_{47}/1000)$	

Note. See spreadsheet model in supporting information. Formulas for calculating ratios for fractional amounts for working gas (WG) or sample CO_2; *R*, ratio = minor species/major species; *F*, fractional amount = species/total. Working gas and samples are processed separately but mainly with the same equations. Separate equations only shown if they are different for a given step. In part from He et al. (2012; see R-code); Huntington et al. (2009; see MATLAB code in their supporting information) and Santrock et al. (1985). Modifications added here include offset for true values for reference gas ($\delta^{13}C_{offset}$ and $\delta^{18}O_{offset}$), excess ^{17}O (Δ_{17}), and excess 47 (Δ_{47}) including effects on ^{13}C, ^{18}O, and ^{16}O pools, and fractional isotopologue absolute abundances (FI_{45}, FI_{46}, and FI_{47}).

Table A2
Generating Model Signal Data From Fractional Amounts

Isotope or mass	Working gas (reference)	Sample
1. 44 mV′	$44\ mV'_{WG} = {}^{44}F_{WG} \times Amp + PBL_{44}$	$44\ mV' = {}^{44}F \times Amp + PBL_{44}$
2. 44Lin		$44Lin = Lin_{44} \times (44\ mV'_{WG} - 44\ mV')$
3. 44 mV	$44mV_{WG} = 44\ mV'_{WG}$	$44\ mV = 44\ mV' \times (1 + 44Lin/1000)$
4. 4XmV′	$4XmV'_{WG} = {}^{4X}F_{WG} \times Amp \times Mult_{4X} + PBL_{4X}$	$4XmV' = {}^{4X}F \times Amp \times Mult_{4X} + PBL_{4X} \times 44\ mV/44\ mV_{WG}$
5. 4XLin		$4XLin = Lin_{4X} \times (4XmV'_{WG} - 4XmV')$
6. 4XmV	$4XmV_{WG} = 4XmV'_{WG}$	$4XmV = 4XmV' \times (1 + 4XLin/1000)$
7. $^{4X}R_{meas}$	$^{4X}R_{WG\text{-}meas} = 4XmV_{WG}/44\ mV_{WG}$	$^{4X}R_{meas} = 4XmV/44\ mV$
8. $^{4X}R_{norm}$	$^{4X}R_{WG\text{-}norm} = {}^{4X}R_{WG\text{-}meas}/{}^{4X}R_{WG\text{-}meas}$	$^{4X}R_{norm} = {}^{4X}R_{meas}/{}^{4X}R_{WG\text{-}meas}$
9. $^{13}R_{WG}$	$^{13}R_{WG} = {}^{13}R_{VPBD'} \times (1 + WG\ \delta^{13}C_{VPDB})$	
10. $^{18}R_{WG}$	$^{18}R_{WG} = {}^{18}R_{VSMOW'} \times (1 + WG\ \delta^{18}O_{VSMOW})$	
11. $^{17}R_{WG}$	$^{17}R_{WG} = K' \times {}^{18}R_{WG}{}^{\lambda'}$	
12. ^{45}R	$^{45}R_{WG} = {}^{13}R_{WG} + 2 \times {}^{17}R_{WG}$	$^{45}R_{sample} = {}^{45}R_{WG} \times {}^{45}R_{norm}$
13. ^{46}R	$^{46}R_{WG} = 2\ x\ {}^{18}R_{WG} + 2 \times {}^{17}R_{WG} \times {}^{13}R_{WG} + {}^{17}R_{WG}{}^2$	$^{46}R_{sample} = {}^{46}R_{WG} \times {}^{46}R_{norm}$
14. **solve**	**Sample processing only**	$0 = -3 \times K^2 \times {}^{18}R^{2\lambda} + 2 \times K \times {}^{45}R \times {}^{18}R^{\lambda} + 2 \times {}^{18}R - {}^{46}R = X$
15. ^{18}R ^{18}O	$^{18}R_{init} = {}^{46}R_{sample}/2.005;\ {}^{18}R_{final} = {}^{18}R_{init} - X/2.0022$	$‰\delta^{18}O_{VSMOW} = 1{,}000 \times (-1 + {}^{18}R_{sample}/{}^{18}R_{VSMOW})$
16. ^{17}R	$^{17}R_{sample} = K \times {}^{18}R^{\lambda}{}_{sample}$	

Table A2
(continued)

Isotope or mass	Working gas (reference)	Sample
17. ^{13}R ^{13}C	$^{13}R_{sample} = {}^{45}R_{sample} - 2 \times {}^{17}R_{sample}$	$‰\delta^{13}C_{VPDB} = 1{,}000 \times ({}^{13}R_{sample} - {}^{13}R_{VPDB})/{}^{13}R_{VPDB}$
18. ^{47}R $^{47}\delta$	$^{47}R_{calc} = 2 \times {}^{18}R_{sample} \times {}^{13}R_{sample} + 2 \times {}^{18}R_{sample} \times {}^{13}R_{sample} + {}^{13}R_{sample} \times {}^{17}R^2_{sample}$	$‰ {}^{47}R_{sample} = 1{,}000 \times (-1 + {}^{47}R_{meas}/{}^{47}R_{WG\text{-}meas})$
19. Δ_{47}	$‰\Delta_{47,\ raw} = 1{,}000 \times ({}^{47}R_{sample} - {}^{47}R_{calc})/{}^{47}R_{calc}$	$‰\Delta_{47,\ sample} = ‰\Delta_{47,\ WG} + ‰\Delta_{47,\ raw}$

Note. See spreadsheet model in supporting information. Formulas for calculating model signal data from fractional amounts for working gas or sample CO_2. F, fractional amount = species/total; Amp, amplitude; mV, signal (millivolts, but any values and relative amplitudes can be used); Mult, multiplier or relative amplification for a given m/z cup. In part from He et al. (2012; see R-code); Huntington et al. (2009; see MATLAB code in their supporting information) and Santrock et al. (1985). Designation "4X" stands for cycling through 45, 46, 47, and 44 as appropriate. For test purposes, $^{13}R_{VPDB'}$, $^{18}R_{VSMOW'}$, K', and λ' values do not have to be the same values used in Table A1 to generate the model data.

Acknowledgments
We would like to thank Bob Clayton for the GISP, VSMOW, and SLAP used in in some of the EG runs, as well as for the turbo pump on our vacuum line. Bo He initially set up our data processing, and Miquela Ingalls provided feedback in the early stages of this project. We would like to thank the reviewers for their time and very useful feedback and Andrew Schauer for discussions at the Clumped Isotope Workshop (Florida). Analyses were done at the Chicago Stable Isotope Ratio facility at the University of Chicago. This work was supported in part by the NSF (EAR-0923831, A. S. C.). Data and Excel model available in supporting information (as Excel worksheets). The authors declare no conflicts of interest from their affiliation or funding.

References

Affek, H. P., & Eiler, J. M. (2006). Abundance of mass 47 CO_2 in urban air, car exhaust, and human breath. *Geochimica et Cosmochimica Acta*, *70*(1), 1–12. https://doi.org/10.1016/j.gca.2005.08.021

Allison, C. E., Francey, R. J., & Meijer, H. A. J. (1995). Recommendations for the reporting of stable isotope measurements of carbon and oxygen in CO_2 gas. In *Reference and intercomparison materials for stable isotopes of light elements*, (pp. 155–162). Vienna, Austria: International Atomic Energy Agency.

Assonov, S. S., & Brenninkmeijer, C. A. M. (2003a). A redetermination of absolute values for 17RVPDB-CO2 and 17RVSMOW. *Rapid Communications in Mass Spectrometry*, *17*(10), 1017–1029. https://doi.org/10.1002/rcm.1011

Assonov, S. S., & Brenninkmeijer, C. A. M. (2003b). On the ^{17}O correction for CO_2 mass spectrometric isotopic analysis. *Rapid Communications in Mass Spectrometry*, *17*(10), 1007–1016. https://doi.org/10.1002/rcm.1012

Baertschi, P. (1976). Absolute18O content of standard mean ocean water. *Earth and Planetary Science Letters*, *31*(3), 341–344. https://doi.org/10.1016/0012-821X(76)90115-1

Barkan, E., & Luz, B. (2005). High precision measurements of $^{17}O/^{16}O$ and $^{18}O/^{16}O$ ratios in H_2O. *Rapid Communications in Mass Spectrometry*, *19*(24), 3737–3742. https://doi.org/10.1002/rcm.2250

Bernasconi, S. M., Hu, B., Wacker, U., Fiebig, J., Breitenbach, S. F. M., & Rutz, T. (2013). Background effects on Faraday collectors in gas-source mass spectrometry and implications for clumped isotope measurements. *Rapid Communications in Mass Spectrometry*, *27*(5), 603–612. https://doi.org/10.1002/rcm.6490

Bernasconi, S. M., Müller, I. A., Bergmann, K. D., Breitenbach, S. F. M., Fernandez, A., Hodell, D. A., et al. (2018). Reducing uncertainties in carbonate clumped isotope analysis through consistent carbonate-based standardization. *Geochemistry, Geophysics, Geosystems*, *19*, 2895–2914. https://doi.org/10.1029/2017GC007385

Brand, W. A., Assonov, S. S., & Coplen, T. B. (2010). Correction for the ^{17}O interference in $\delta(^{13}C)$ measurements when analyzing CO_2 with stable isotope mass spectrometry (IUPAC Technical Report). *Pure and Applied Chemistry*, *82*(8), 1719–1733. https://doi.org/10.1351/PAC-REP-09-01-05

Chang, T. L., & Li, W. (1990). A calibrated measurement of the atomic weight of carbon. *Chinese Science Bulletin*, *35*(4), 290–296.

Coplen, T. B., Böhlke, J. K., De, B. P., Ding, T., Holden, N. E., Hopple, J. A., et al. (2002). Isotope-abundance variations of selected elements (IUPAC Technical Report). *Pure and Applied Chemistry*, *74*(10), 1987–2017. https://doi.org/10.1351/pac200274101987

Craig, H. (1953). The geochemistry of the stable carbon isotopes. *Geochimica et Cosmochimica Acta*, *3*(2-3), 53–92. https://doi.org/10.1016/0016-7037(53)90001-5

Daëron, M., Blamart, D., Peral, M., & Affek, H. P. (2016). Absolute isotopic abundance ratios and the accuracy of Δ47 measurements. *Chemical Geology*, *442*, 83–96. https://doi.org/10.1016/j.chemgeo.2016.08.014

Davies, A. J., & John, C. M. (2017). Reducing contamination parameters for clumped isotope analysis: The effect of lowering Porapak™ Q trap temperature to below −50 °C. *Rapid Communications in Mass Spectrometry*, *31*(16), 1313–1323. https://doi.org/10.1002/rcm.7902

Dennis, K. J., Affek, H. P., Passey, B. H., Schrag, D. P., & Eiler, J. M. (2011). Defining an absolute reference frame for 'clumped' isotope studies of CO_2. *Geochimica et Cosmochimica Acta*, *75*(22), 7117–7131. https://doi.org/10.1016/j.gca.2011.09.025

Eiler, J. M. (2007). "Clumped-isotope" geochemistry—The study of naturally-occurring, multiply-substituted isotopologues. *Earth and Planetary Science Letters*, *262*(3–4), 309–327. https://doi.org/10.1016/j.epsl.2007.08.020

Eiler, J. M., Bergquist, B., Bourg, I., Cartigny, P., Farquhar, J., Gagnon, A., et al. (2014). Frontiers of stable isotope geoscience. *Chemical Geology*, *372*, 119–143. https://doi.org/10.1016/j.chemgeo.2014.02.006

Eiler, J. M., & Schauble, E. (2004). 18O13C16O in Earth's atmosphere. *Geochimica et Cosmochimica Acta*, *68*(23), 4767–4777. https://doi.org/10.1016/j.gca.2004.05.035

Farquhar, J., Thiemens, M. H., & Jackson, T. (1998). Atmosphere-Surface Interactions on Mars: Δ17O Measurements of Carbonate from ALH 84001. *Science*, *280*(5369), 1580–1582. https://doi.org/10.1126/science.280.5369.1580

Fernandez, A., Müller, I. A., Rodríguez-Sanz, L., van Dijk, J., Looser, N., & Bernasconi, S. M. (2017). A Reassessment of the precision of carbonate clumped isotope measurements: Implications for calibrations and paleoclimate reconstructions. *Geochemistry, Geophysics, Geosystems*, *18*, 4375–4386. https://doi.org/10.1002/2017GC007106

Fiebig, J., Hofmann, S., Löffler, N., Lüdecke, T., Methner, K., & Wacker, U. (2016). Slight pressure imbalances can affect accuracy and precision of dual inlet-based clumped isotope analysis. *Isotopes in Environmental and Health Studies*, *52*(1–2), 12–28. https://doi.org/10.1080/10256016.2015.1010531

Ghosh, P., Adkins, J., Affek, H., Balta, B., Guo, W., Schauble, E. A., et al. (2006). 13C–18O bonds in carbonate minerals: A new kind of paleothermometer. *Geochimica et Cosmochimica Acta*, *70*(6), 1439–1456. https://doi.org/10.1016/j.gca.2005.11.014

Gonfiantini, R., Stichler, W., & Rozansk, K. (1995). Standards and intercomparison materials distributed by the International Atomic Energy Agency for stable isotope measurements. In *Reference and Intercomparison Materials for Stable Isotopes of Light Elements*, (pp. 13–29). Vienna, Austria: International Atomic Energy Agency.

Halevy, I., Fischer, W. W., & Eiler, J. M. (2011). Carbonates in the Martian meteorite Allan Hills 84001 formed at 18 ± 4 °C in a near-surface aqueous environment. *Proceedings of the National Academy of Sciences*, *108*(41), 16,895–16,899. https://doi.org/10.1073/pnas.1109444108

He, B., Olack, G. A., & Colman, A. S. (2012). Pressure baseline correction and high-precision CO_2 clumped-isotope (Δ47) measurements in bellows and micro-volume modes. *Rapid Communications in Mass Spectrometry*, *26*(24), 2837–2853. https://doi.org/10.1002/rcm.6436

Hu, B., Radke, J., Schlüter, H.-J., Heine, F. T., Zhou, L., & Bernasconi, S. M. (2014). A modified procedure for gas-source isotope ratio mass spectrometry: The long-integration dual-inlet (LIDI) methodology and implications for clumped isotope measurements. *Rapid Communications in Mass Spectrometry*, *28*(13), 1413–1425. https://doi.org/10.1002/rcm.6909

Huntington, K. W., Eiler, J. M., Affek, H. P., Guo, W., Bonifacie, M., Yeung, L. Y., et al. (2009). Methods and limitations of 'clumped' CO_2 isotope (Δ47) analysis by gas-source isotope ratio mass spectrometry. *Journal of Mass Spectrometry*, *44*(9), 1318–1329. https://doi.org/10.1002/jms.1614

Kaiser, J. (2008). Reformulated ^{17}O correction of mass spectrometric stable isotope measurements in carbon dioxide and a critical appraisal of historic 'absolute' carbon and oxygen isotope ratios. *Geochimica et Cosmochimica Acta*, *72*(5), 1312–1334. https://doi.org/10.1016/j.gca.2007.12.011

Landais, A., Barkan, E., & Luz, B. (2008). Record of $\delta^{18}O$ and ^{17}O-excess in ice from Vostok Antarctica during the last 150,000 years. *Geophysical Research Letters*, *35*, L02709. https://doi.org/10.1029/2007GL032096

Li, W., Ni, B., Jin, D., & Zhang, Q. (1988). Measurement of the absolute abundance of O-17 in V-Smow. *Kexue Tongbao*, *33*(19), 1610–1613.

Luz, B., & Barkan, E. (2010). Variations of $^{17}O/^{16}O$ and $^{18}O/^{16}O$ in meteoric waters. *Geochimica et Cosmochimica Acta*, *74*(22), 6276–6286. https://doi.org/10.1016/j.gca.2010.08.016

Matsuhisa, Y., Goldsmith, J. R., & Clayton, R. N. (1978). Mechanisms of hydrothermal crystallization of quartz at 250 °C and 15 kbar. *Geochimica et Cosmochimica Acta*, *42*(2), 173–182. https://doi.org/10.1016/0016-7037(78)90130-8

Meijer, H. A. J., & Li, W. J. (1998). The use of electrolysis for accurate $\delta^{17}O$ and $\delta^{18}O$ isotope measurements in water. *Isotopes in Environmental and Health Studies*, *34*(4), 349–369. https://doi.org/10.1080/10256019808234072

Mook, W. G., & Grootes, P. M. (1973). The measuring procedure and corrections for the high-precision mass-spectrometric analysis of isotopic abundance ratios, especially referring to carbon, oxygen and nitrogen. *International Journal of Mass Spectrometry and Ion Physics*, *12*(3), 273–298. https://doi.org/10.1016/0020-7381(73)80044-0

Müller, I. A., Fernandez, A., Radke, J., van Dijk, J., Bowen, D., Schwieters, J., & Bernasconi, S. M. (2017). Carbonate clumped isotope analyses with the long-integration dual-inlet (LIDI) workflow: Scratching at the lower sample weight boundaries. *Rapid Communications in Mass Spectrometry*, *31*(12), 1057–1066. https://doi.org/10.1002/rcm.7878

Nier, A. O. (1950). A redetermination of the relative abundances of the isotopes of carbon, nitrogen, oxygen, argon, and potassium. *Physical Review*, *77*(6), 789–793. https://doi.org/10.1103/PhysRev.77.789

Olack, G., & Colman, A. (2016). Influence of ^{17}O correction parameters on calculation and calibration of Δ47. Presented at the Goldschmidt Conference, 2016, Yokohama, Japan. Retrieved from https://goldschmidtabstracts.info/2016/2378.pdf

Olack, G., He, B., & Colman, A. (2013). Corrections for ^{17}O interference, effects on Δ47 determination. Poster presented at the AGU 2013 Fall Meeting, San Francisco, CA. Retrieved from. http://abstractsearch.agu.org/meetings/2013/FM/V53B-2772.html

Ross, S. M. (2003). Peirce's criterion for the elimination of suspect experimental data. *Journal of Engineering Technology*, (2), 1–12.

Santrock, J., Studley, S. A., & Hayes, J. M. (1985). Isotopic analyses based on the mass spectra of carbon dioxide. *Analytical Chemistry*, *57*(7), 1444–1448. https://doi.org/10.1021/ac00284a060

Schauer, A. J., Kelson, J., Saenger, C., & Huntington, K. W. (2016). Choice of ^{17}O correction affects clumped isotope (Δ47) values of CO_2 measured with mass spectrometry. *Rapid Communications in Mass Spectrometry*, *30*(24), 2607–2616. https://doi.org/10.1002/rcm.7743

Wang, Z., Schauble, E. A., & Eiler, J. M. (2004). Equilibrium thermodynamics of multiply substituted isotopologues of molecular gases. *Geochimica et Cosmochimica Acta*, *68*(23), 4779–4797. https://doi.org/10.1016/j.gca.2004.05.039

Westley, M. B., Popp, B. N., & Rust, T. M. (2007). The calibration of the intramolecular nitrogen isotope distribution in nitrous oxide measured by isotope ratio mass spectrometry. *Rapid Communications in Mass Spectrometry*, *21*(3), 391–405. https://doi.org/10.1002/rcm.2828

Yeung, L. Y., Young, E. D., & Schauble, E. A. (2012). Measurements of $^{18}O^{18}O$ and $^{17}O^{18}O$ in the atmosphere and the role of isotope-exchange reactions. *Journal of Geophysical Research*, *117*, D18306. https://doi.org/10.1029/2012JD017992

Zhang, Q., & Li, W. (1987). Mass spectrometric determination of the absolute isotopic abundance of carbon in NBS-20. Proc. 2nd Beijing Conf. and Exhib. on Instrum. Analysis, 391–392.